International Journal of Earth Sciences
https://doi.org/10.1007/s00531-024-02428-4

ORIGINAL PAPER

Organic geochemistry of Palaeogene coals from Greenland and Svalbard

Franz Philip Kerschhofer[1,3] · Martin Blumenberg[2] · Jolanta Kus[2] · Lutz Reinhardt[2] · Volker Thiel[1]

Received: 3 November 2023 / Accepted: 10 May 2024

Abstract

The organic geochemistry and coal petrology of Palaeogene coals from northeast Greenland (Thyra Ø Island and Kronprins Christian Land) and central Spitsbergen (Longyearbyen and Grumantbyen) were studied using Rock–Eval and gas chromatography–mass spectrometry, as well as microphotometry and maceral group analyses. Bulk data and biomarker distributions of the coals demonstrate a low coal rank for both, but a lower coalification degree of coals from Greenland (0.49–0.55% VRr) compared to those from Svalbard (0.68–0.75% VRr). Maceral group analyses revealed relatively similar distributions with a strong predominance of vitrinite. The generally high abundance of hopanoids (hopanes/hopenes and hopanoic acids) implies a strong bacterial reworking of the organic matter, whereas sulphur occurrences indicate a marine influence after organic matter deposition. A great variety of higher plant biomarkers was detected in all coals. Distinctive compounds recorded in the coals are aliphatic and aromatic diterpenoids as well as partly hydrogenated picenes, suggesting strong input of conifers and angiosperms. Pristane/phytane ratios indicate that the organic matter in the ancient swamps was deposited in an oxic, fluvio-deltaic setting at both sites. This study provides a detailed geochemical investigation of understudied coals from northeast Greenland. Moreover, it enhances our understanding of probably interrelated Palaeogene depositional settings from Greenland and Spitsbergen in terms of their palaeoecology, primary input into coal swamps, and individual thermal history.

Keywords Coals · Svalbard and Greenland · Lipid biomarkers · Terpenoids · Arctic · Palaeogene

Introduction

On the early Paleogene Earth, warm greenhouse conditions prevailed and rainforests reached as far north as the Arctic Circle (Greenwood et al. 2010; Myhre and Eldholm 1988; Ruddiman 2014; Weijers et al. 2007; West et al. 2015). With average air temperatures on land of about 17 °C (Weijers et al. 2007), these conditions were ideal for the formation of coal swamps (Greenwood et al. 2010; Sluijs et al. 2006). A wide range of macrofossils documents the occurrence of different higher plants at high northern latitudes (Dolezych et al. 2019). In the palaeoarctic environments that once existed in Greenland and Spitsbergen (main island of the Svalbard Archipelago), a mosaic of landscapes existed, with rich deciduous conifers growing in lowland swamps and poorly drained basins of floodplains, and various angiosperms at drier sites (Schlanser et al. 2020 and references therein). The warm and wet climate supported high productivity (Boyd 1990; Dolezych et al. 2019) while the conditions during the winter were still bearable for the plants to survive the lack of light (Schweitzer 1980). *Metasequoia occidentalis* is one of the most abundant conifers (Schweitzer 1980) while typical vegetation also includes *Cunninghamia*, *Glyptostrobus*, *Dennstaedtia*, *Ginkgo*, other Metasequoia species, *Cercidiphyllum* and *Platanus* (Boyd 1990; Dolezych et al. 2019).

At the beginning of the Palaeogene, Greenland and Spitsbergen were part of the Laurasian continental platform

✉ Franz Philip Kerschhofer
fp.kerschhofer@gmail.com

[1] Geobiology, Geoscience Centre, University of Göttingen, Goldschmidtstr. 3, 37077 Göttingen, Germany

[2] Federal Institute for Geosciences and Natural Resources (BGR), Stilleweg 2, 30655 Hannover, Germany

[3] Present Address: ETH Zurich, Zurich, Switzerland

Published online: 17 July 2024

(Blythe and Kleinspehn 1998; Faleide et al. 1993; Lawver et al. 1990; Fig. 1a). At this time, plate tectonic processes led to the final opening of the North Atlantic and its connection with the Arctic Ocean (Dallmann 2015; Piepjohn et al. 2016; Tessensohn and Piepjohn 2000). South of Greenland, rift branches initially caused transpressive forces between northeast Greenland and Spitsbergen (Eurekan deformation, e.g., Piepjohn et al. 2016; Tessensohn and Piepjohn 2000; Fig. 1b). Later, directional changes of Greenland led to changing stress regimes and caused the separation of Greenland and Spitsbergen by the formation of the Greenland-Norwegian Seas via a transform and/or strike-slip movements (Blythe and Kleinspehn 1998; Lawver et al. 1990; Piepjohn et al. 2016).

In this context, sedimentary basins formed, which were situated at similar latitudes as today, namely the Wandel Sea Basin in north-eastern Greenland and the Central Tertiary Basin (CTB) in central Spitsbergen (Bruhn and Steel 2003; Lyck and Stemmerik 2000; Fig. 1b and Fig. 2a).

In Greenland, the coal-bearing Wandel Sea Basin existed from the Carboniferous to the Tertiary. It crops out in modern north-eastern Greenland (Lyck and Stemmerik 2000). The youngest preserved sediments are dated as Palaeogene deposits (late Palaeocene to possibly early Eocene) and contain the coal seams investigated in this study (Stemmerik et al. 1998). These sediments of the Thyra Ø Formation are mostly rarely affected by deformation and are generally characterised by flat-lying strata (Paech and Estrada 2019, Fig. 2b). The base of the Thyra Ø Formation is unknown. The formation is uncomformably underlying Quaternary marine deposits and is generally poorly exposed at the surface; most information is derived from isolated outcrops. The fine-grained sandstones, organic-poor siltstones and coals of the Thyra Ø Formation have an estimated composite thickness of 50 m (Håkansson et al. 1991; Lyck and Stemmerik 2000). On Prinsesse Thyra Ø Island, coal seams have a thickness of less than 30 cm (Paech and Estrada 2019). Recently, Piasecki et al. (2018) identified Lower to Middle Eocene marginal marine deposits on Kap Rigsdagen unconformably overlying Barremian sandstones there.

On the Spitsbergen side, the Palaeogene deposits of the CTB, collectively called the Van Mijenfjorden Group, range from the early Palaeocene probably up into the Oligocene, based on palynological data and other macrofossils (Blythe and Kleinspehn 1998 and references therein) as well as on

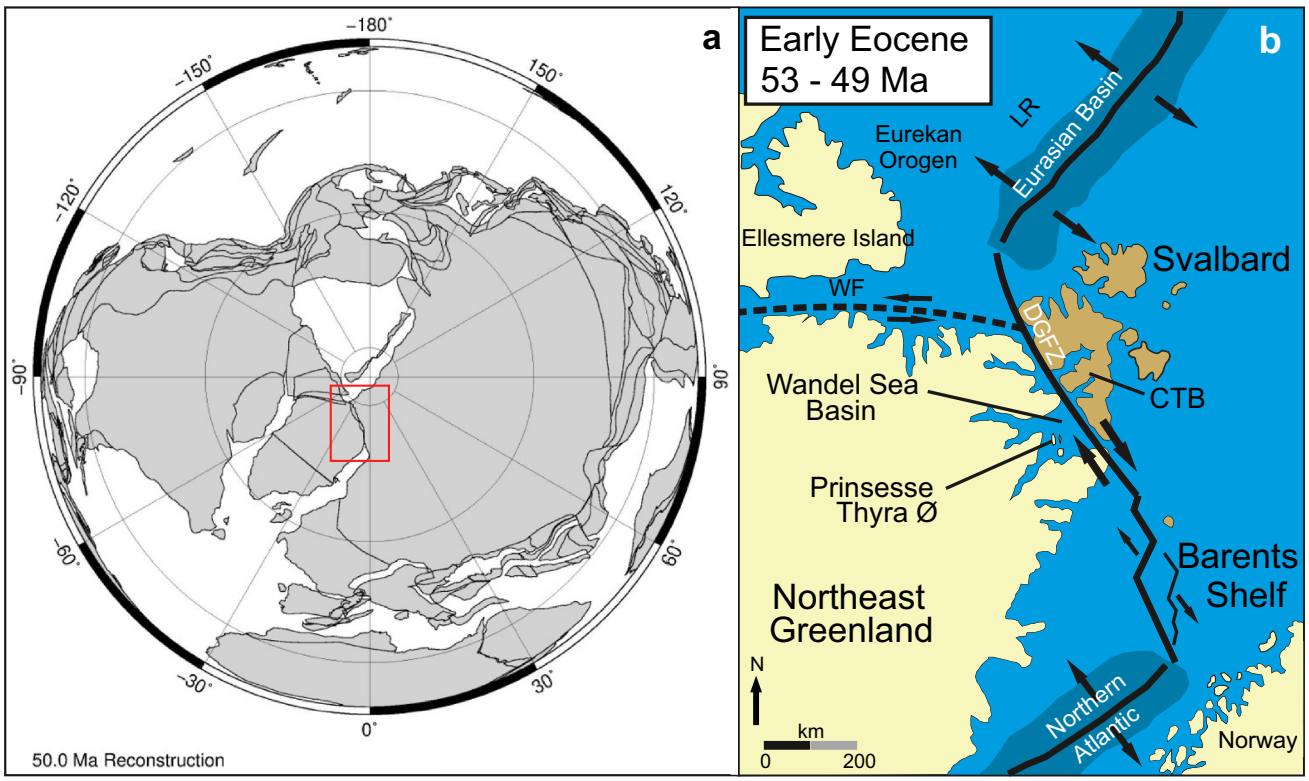

Fig. 1 Palaeogeographic overview. **a** Palaeogeographic reconstruction of the northern hemisphere at 50 Ma (map created with ODSN 2022). Black lines on the continents represent plate boundaries; red square marks the area of the map shown in b; **b** Outline of the main tectonic structures and movements during the Early Eocene in the area between North-eastern Greenland and Svalbard (after Blumenberg et al. 2019 and Blythe and Kleinspehn 1998). *LR* Lomonosov Ridge, *WF* Wegener Fault, *DGFZ* De Geer Fracture Zone, *CTB* Central Tertiary Basin

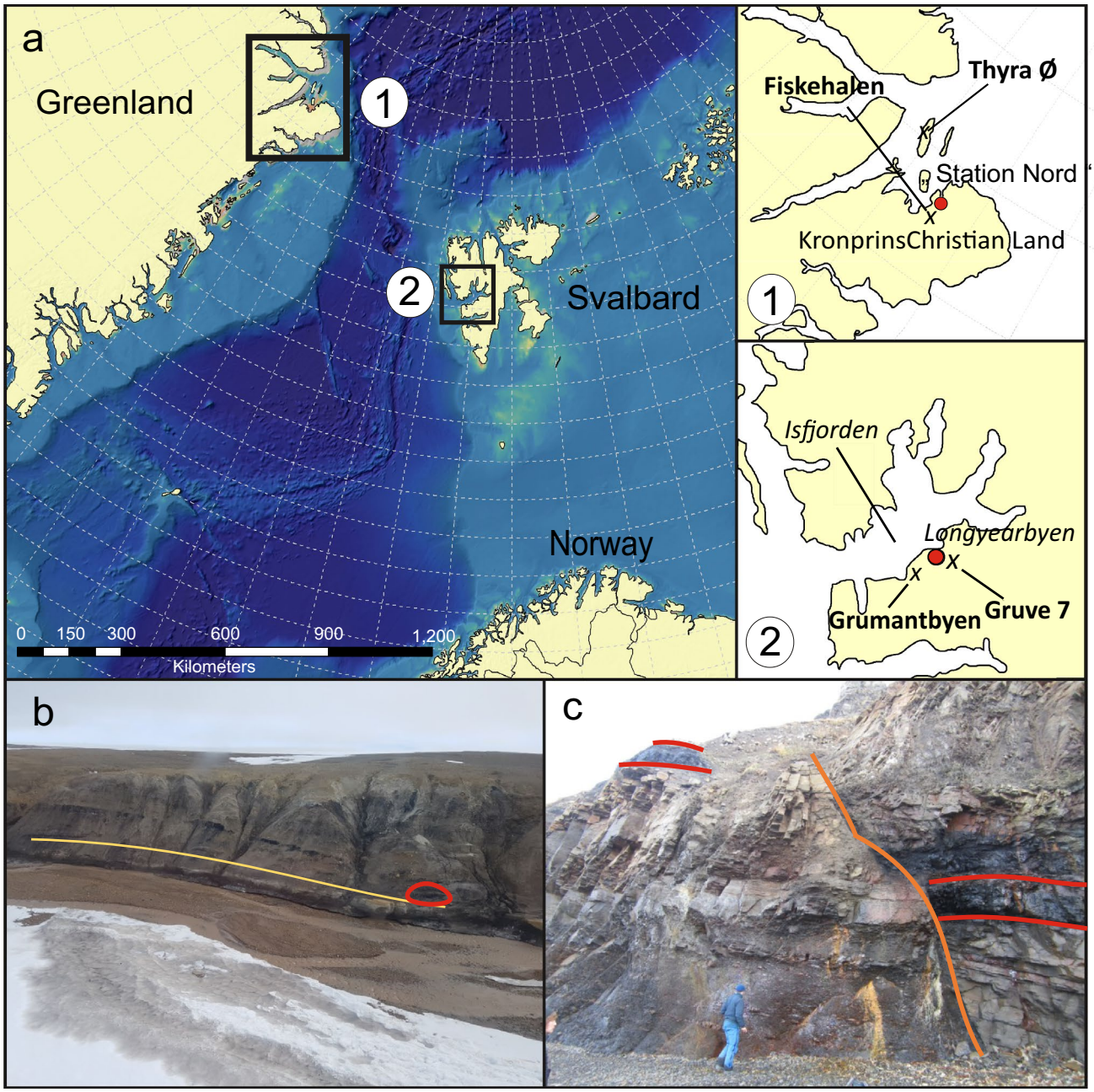

Fig. 2 Maps and photos of the study sites in Greenland and Spitsbergen. **a** Map of the present position of Greenland and Spitsbergen with rectangles indicating the sampling areas in Greenland (1) and Spitsbergen (2), respectively. Inset 1 illustrates the positions of outcrops Fiskehalen and Prinsesse Thyra Ø Island. Inset 2 illustrates the positions of the outcrop at Grumantbyen and at coal mine Gruve 7 on Svalbard. Map after Blumenberg et al. 2019. **b** Photo of the outcrop Fiskehalen, view to the ~ northeast. The yellow line marks a prominent sandstone at the base of the outcrop, overlain by the sampled coal seam. The red circle marks the sampling position of sample Green1. The outcrop length is approximately 40 m. **c** Photo of the outcrop near Grumantbyen, situated directly at the coastline where sample Spits2 was taken from the prominent coal seam. The orange line marks a normal fault. The red lines enhance the visibility of the coal seam, which has been offset by the normal fault (person for scale). The maps were created with esri ArcGis (NOAA 2019)

U–Pb dating of zircons derived from volcanic ash layers preserved as bentonites (Charles et al. 2011; Elling et al. 2016; Jochmann et al. 2020; Jones et al. 2016, 2017). The sediments exceed 1900 m in thickness and consist mainly of sandstones, conglomerates, siltstones, claystones and coals (Ćmiel and Fabiańska 2004; Elling et al. 2016 and references therein). Close to the unconformity separating the Van Mijenfjorden Group from underlying Cretaceous strata, three to five coal seams occur in the Firkanten Formation with thicknesses ranging from 0.5 to 5 m (Elling et al.

2016; Orheim et al. 2007; Fig. 2c). Based on recent age determinations of zircon grains preserved in bentonite layers of the Firkanten Fm., Jones et al. (2016, 2017) suggested that sedimentation in the eastern CTB began at about 61.8 Ma, i.e. at the Danian/Selandian boundary. The coal samples investigated here were collected from the lowermost coal seam located just above the unconformity (see Fig. 2c, for further stratigraphical description and information see Ćmiel and Fabiańska 2004, Elling et al. 2016, Jochmann et al. 2020 and Marshall et al. 2015b).

A more detailed correlation of the stratigraphy between Greenland and Spitsbergen is not possible so far, as probable volcanic ash layers in the Palaeogene sediments from Greenland have been identified only recently (Paech and Estrada 2019). Hence, the chronology of the Thyra Ø Formation is entirely based on sedimentological interpretations and biostratigraphy (Lyck and Stemmerik 2000; Piasecki et al. 2018) which can, however, only give a general time frame of the deposition from Palaeocene to Late Palaeocene or possibly early Eocene to Middle Eocene. Moreover, it is not clear whether the same depositional facies developed in Greenland and Spitsbergen during the exact same time periods.

Palaeocene coals from Spitsbergen have already been investigated in detail (Blumenberg et al. 2019, Ćmiel and Fabiańska 2004; Marshall et al. 2015b; BGR Arctic Viewer 2021), but age-equivalent coals from Greenland are understudied with respect to their organic geochemistry, palaeoecology, primary input, and individual coalification. In this study, we use biomarkers and coal petrographic parameters for comparison and reconstruction of palaeo-settings and coalification. Biomarkers are molecular remnants of lipids found in sedimentary environments (Peters et al. 2005). These compounds were derived from e.g. leaf surface lipids, cell membranes, and other natural products, and are ultimately transformed to hydrocarbons which can endure for millions and even billions of years. Their carbon skeletons often still mirror the original lipids from their biological precursors (Peters et al. 2005). Our study thus provides new insights into the environmental conditions that once prevailed in these likely connected arctic settings of the Palaeogene greenhouse world.

Materials and methods

Sampling

Three samples from central Spitsbergen were collected from natural outcrops located on the southern margin of the Isfjorden during BGR expedition CASE 17–2 in August/September 2015 (sample prefix "Spits") and during a visit in the Gruve 7 coal mine. Another three samples from NE Greenland (sample prefix "Green") were taken from natural outcrops at Fiskehalen on Kronprins Christian Land and at Prinsesse Thyra Ø Island during BGR expedition CASE-20 in July 2018 (Fig. 2a). Exact coordinates (acquired by handheld GPS, error ± 5 m) are given in Table 1.

The Greenland coals were collected from seams within the Palaeogene (Late Palaeocene to Early Eocene) Thyra Ø Formation (Lyck and Stemmerik 2000). The coal of Fiskehalen (Green1) was sampled in a river valley from a natural steep outcrop of approximately 30 m in height. Figure 2b gives an overview of this outcrop. Within alternating layers of sand and six coal seams, the investigated coal was sampled from the lowermost coal seam overlying a prominent sandstone unit at the base of the outcrop. Coals from Prinsesse Thyra Ø (Green2a and Green2b) were sampled along a natural outcrop along the outside bank of a small river; Green2a is located more inland, about 700 m east of Green2b. The shallow inclination of the bedding is in an eastward direction, indicating a somewhat younger age for Green2a.

All samples from Spitsbergen belong to the Firkanten Formation, the stratigraphically oldest unit of Van Mijenfjorden Group that further comprises the Basilika/Grumantbyen/Frysjaodden/Battfjellet/Aspelintoppen Formations within the CTB. In the active coal mine Gruve 7 near Longyearbyen, two coal samples were taken in a mine section from the top (Spits1a) and the bottom (Spits1b) of the seam. A third sample was obtained at the abandoned coal mine of Grumantbyen from the lowermost coal seam cropping out at a 20 m high section along the shoreline (Spits2, Fig. 2c).

Bulk geochemistry

Aliquots of dried (40 ℃ for 24 h) coal samples were ground and used for bulk analyses. Total organic carbon (TOC) and carbonate carbon (Ccarb) as well as sulphur concentrations were analysed using a LECO CS-230 analyser (Leco Instrumente, Germany). TOC was determined on decalcified (10% HCl at 80 ℃; dried at 40 ℃ for 18 h) sample aliquots (10–40 mg) and Ccarb was calculated from the difference between the data for TOC and total carbon. The instrument was calibrated using LECO standards and the reproducibility of the measurements was ± 0.02%. Rock–Eval pyrolysis was performed on a Rock–Eval 6 analyser using a standard programme (Espitalié et al. 1977; Lafargue et al. 1998). The reproducibility of the hydrocarbons and CO_2 determination was better than 5%.

Coal petrology

The samples were dried in a nitrogen-flushed oven at a temperature of 25 °C and subsequently crushed to obtain the < 1 mm fraction for coal petrographic analysis. Coal

Table 1 Sample codes and locations

Sample code	Green1	Green2a	Green2b	Spits1a	Spits1b	Spits2
Age	Late Palaeocene[b]	Late Palaeocene[b]	Late Palaeocene[b]	Palaeocene[a]	Palaeocene[a]	Palaeocene[a]*
Outcrop/region	Riverbed, Fiskehalen	Riverbed, Thyra Ø	Riverbed, Thyra Ø	Mine Gruve 7, Longyearbyen	Mine Gruve 7, Longyearbyen	Coast, Grumantbyen
Longitude[c]	− 16.94542	− 19.08771	− 19.12953	16.0273	16.0273	15.08836
Latitude[c]	81.42347	81.87534	81.87253	78.1577	78.1577	78.17167

[a]Ages from Elling et al. (2016), Jones et al. (2016, 2017)

[b]Ages fromLyck and Stemmerik (2000)

[c]Lat/Lon WGS84

*Spits2 is likely Danian/Selandian

pellets were prepared following a dry grinding and polishing technique developed by Bertrand Ligouis, LAOP, Tübingen, Germany (see Gorbanenko 2017 and ISO 7404–2 2009 for details; the final polishing was performed with abrasive of maximum size at 0.05 µm). Random vitrinite reflectance measurements were conducted on a Leica DMRX incident light microscope with MPV-Combi Photomultiplier System under the following conditions: non-drying oil immersion $n_{e(546\ nm)} = 1.518$, wavelength of 546 nm, and temperature of 23 ± 1 ℃ in accordance to ISO 7404–3 (2009) and methods described in Taylor et al. (1998). The size of the measuring diaphragm is 2×2 µm. The random vitrinite reflectance was performed in accordance with DIN 22020–5 (2005), analogous to standard ISO 7404–5 (2009). Detailed maceral group analysis was conducted in accordance with DIN 22020–3 (1998), analogous to standard ISO 7404–3 (2009) and methods described in Taylor et al. (1998). The identification and characterization of the coaly matter followed the ICCP nomenclature (ICCP 1998, 2001; Pickel et al. 2017).

The Tissue Preservation Index (TPI) and Gelification Index (GI) follow the formula suggested by Kalaitzidis et al. (2000):

$$TIP = \frac{\text{Humotelinite} + \text{Corhuminite} + \text{Fusinite} + \text{Semifusinite}}{\text{Attrinite} + \text{Densinite} + \text{Gelinite} + \text{Inertodetrinite}}$$

$$GI = \frac{\text{Ulminite} + \text{Geloguminite} + \text{Densinite}}{\text{Textinite} + \text{Atrinite} + \text{Inertinite}}$$

The TPI vs. GI diagram allows us to provide information on the palaeoenvironmental conditions during peat formation. TPI is defined as a ratio of tissue-derived structure to structureless macerals and a measure of the humification grade of the initial organic matter (Kus et al. 2020). On the other hand, the Gelification Index (GI) is the calculated ratio of the gelified to the non-gelified macerals and a measure of moisture conditions on the palaeomire surface (Kus et al. 2020).

Biomarker analysis

Pre-heated sea sand was used as a preparation blank to keep track of contamination throughout the entire analytical process. The samples (0.5 g) were crushed into powder, extracted with 5 ml dichloromethane (DCM)/methanol (MeOH) (3:1, v:v) under ultrasonication (30 min, 40 °C), and centrifuged. Extraction was repeated with 5 ml DCM and 5 ml of *n*-hexane. The extracts were combined, and the resulting total organic extract (TOE) was blown to near-dryness with nitrogen at 40 ℃.

For the separation of maltene and asphaltene fractions, a large surplus of cold *n*-pentane (~10 ml, 6 ℃) was added to the TOEs (dissolved in 1.5 mL DCM) which were then centrifuged (2000 rpm, 15 min). To enhance the visibility of the *n*-pentane/DCM phase separation, one to two drops of highly pure and deionised water ("Milipore-grade") were added. The *n*-pentane phase containing the maltene fractions was reduced to ca. 3 ml (N_2, 40 ℃), and HCl-activated copper was added for desulphurisation (24 h). Aliquots (50%) of the maltenes were fractionated into aliphatic and aromatic hydrocarbons using column chromatography (15 mm i.d., 30 cm length). The samples were dried onto 0.5 g of silica gel and placed on top of the column filled with 7 g Merck silica gel 60. The following sequence of organic solvents were used for elution; 27 ml *n*-hexane for aliphatic hydrocarbons (fraction 1, F1); 32 ml *n*-hexane:DCM (1:1, v:v) for aromatic hydrocarbons (F2); 40 ml DCM:MeOH (1:1, v:v) for the polar fraction (F3). F1 and F2 were analysed by gas chromatography-mass spectrometry (GC–MS; for GC–MS parameters see Supplementary Table 1). Carboxylic acids contained in the F3 fractions were esterified using trimethylchlorosilane (TMCS)/MeOH (1:9, v:v; 90 min, 80 ℃). After cooling, the resulting methyl esters were extracted from the reaction mixture three times with 0.5 ml portions of *n*-hexane. The combined extracts were dried (N_2, 40 °C) and analysed with GC–MS (parameter details can be found in Supplementary Table 1). Appropriate internal standards

were used for quantification (F1, *n*-icosane D_{42}; F2, Ehrenstorf PAH mix Iso 17,034; F3, *n*-nonadecanoic acid methyl ester).

Results

Coal petrology and bulk organic matter

All studied coals showed TOC contents > 65 wt. % and varying sulphur contents ranging from 0.5 to 2.2 wt. % (Table 2). Rock–Eval analyses demonstrated lower T_{max} values for Palaeogene coals from NE Greenland (411–425 ℃) than for Palaeocene coals from Svalbard (436–441 ℃). Hydrogen indices (HI) were relatively high and vice versa oxygen indices were low for all studied coals.

The mean random VRr values of vitrinite in polished coal pellets from NE Greenland ranged from 0.49 and 0.59% (Table 2). All vitrinites showed a high qualifier advocating high reliability of the reflectance measurements. This is further supported by the low standard deviation. Coal samples from Spitsbergen revealed greater random vitrinite reflectance values ranging between 0.69 and 0.75% VRr and were likewise associated with a high qualifier. The mean vitrinite reflectance corresponds to highly volatile bituminous coals.

Additionally, maceral group compositions were analysed for three samples (Green1, Spits1a, Spits1b; Table 2, Fig. 3). The maceral compositions are strongly dominated by vitrinite (> 85%) and additionally contain inertinite and liptinite in comparable abundances (< 10%). The TPI and GI values (≥ 1; 2.8 for both parameters) were obtained solely for Green1 sample and suggest a dominance of xylite-rich samples with a relatively higher degree of preservation. This is in agreement with a low inertinite content, indicating water-saturated depositional conditions preventing organic matter from the oxidative processes. Higher telovitrinite content in Spitsbergen coals can imply a higher contribution of wood from gymnosperms (e.g., O'Keefe et al. 2013).

Major compound classes in extracts

Whereas total amounts of extractable compounds were similar in coals from both regions (932–1545 µg/g TOC, Fig. 4), there were notable differences in the compound class distributions (Fig. 4). In the Greenland coals, fatty acids accounted for the largest relative proportion (~ 60%). Aromatics were the second largest fraction. In the coals from Spitsbergen, aromatics were the main compounds (48–80%), followed by aliphatic hydrocarbons. Here, only traces of fatty acids were present.

Aliphatic hydrocarbons

n-Alkanes

n-Alkanes with carbon chain lengths from *n*-C_{14} to *n*-C_{33} were abundant in all coals (Fig. 5, concentrations in Supplementary Table 2). The Greenland coals varied in their *n*-alkane distributions. Green2b had unimodal (max at *n*-C_{23}) whereas Green1 (maxima at *n*-C_{25} and *n*-C_{31}) and Green2a (maxima at *n*-C_{23} and *n*-C_{29}) had bimodal distributions of *n*-alkanes (Fig. 5a). All coals from Spitsbergen showed an unimodal *n*-alkane distribution with a maximum at *n*-C_{23} (Fig. 5b). The Greenland coals had a strong odd-over-even carbon chain length predominance (OEP) for medium- and long-chain *n*-alkanes (OEP $C_{21\text{-}25}$ 2.4–3.1, CPI $C_{23\text{-}33}$ 1.8–3.0), while coals from Spitsbergen showed a less pronounced OEP, associated with lower CPI (OEP

Table 2 Bulk geochemical (Rock–Eval und Leco C/S) and coal petrological results

Sample		Green1	Green2a	Green2b	Spits1a	Spits1b	Spits2
Rock–Eval	T_{max} (°C)	411	422	425	440	441	436
	HI	265	279	351	396	316	292
	OI	10	8	7	4	1	1
Leco C/S (wt. %)	TOC	68.8	72.3	74.1	76.2	78.7	76.7
	S	0.7	0.7	2.2	0.5	2.1	2
Maceral composition (%)	Vitr	88	NA	NA	86	88	NA
	Lipt	7	NA	NA	9	5	NA
	Inert	5	NA	NA	2	5	NA
	Miner	0	NA	NA	3	2	NA
	TPI	2.8	NA	NA	NA	NA	NA
	GI	2.8	NA	NA	NA	NA	NA
Reflectance	VRr %	0.53	0.59	0.49	0.69	0.68	0.75
	Rc%	0.5	0.6	0.6	0.7	0.7	0.6

NA not available

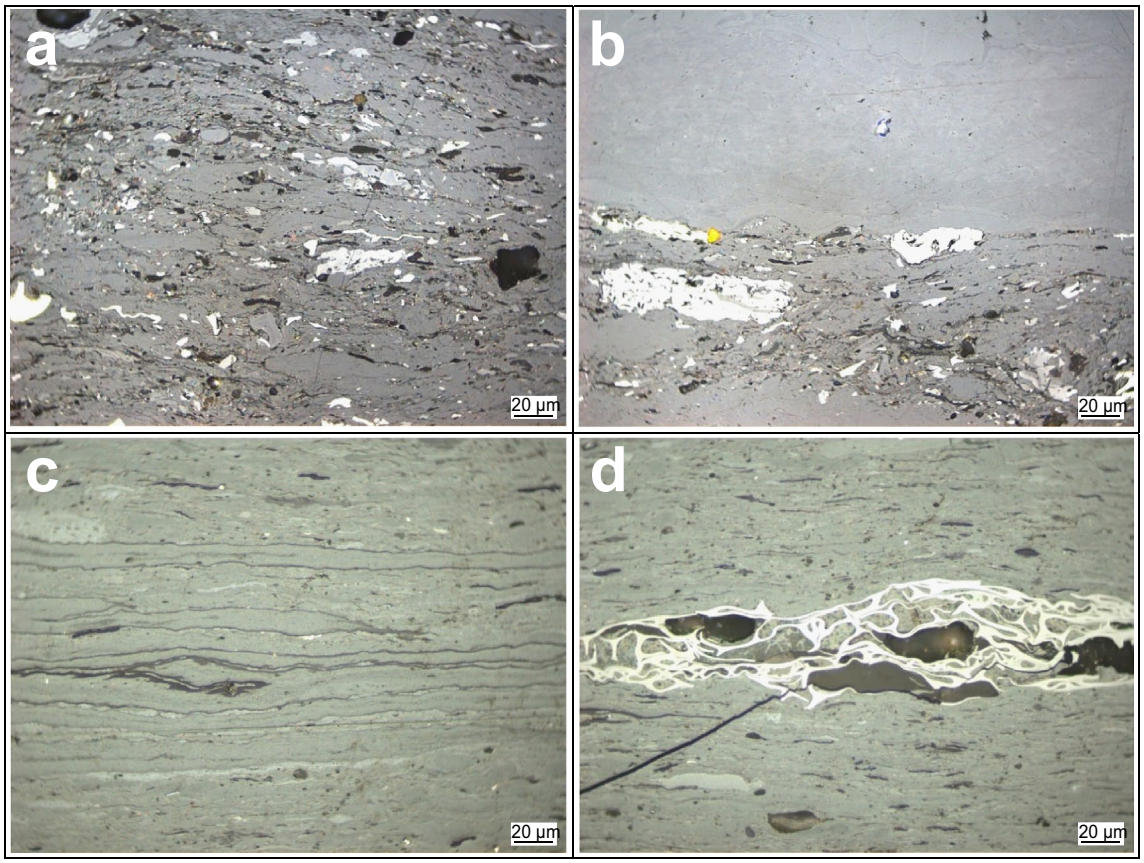

Fig. 3 Microphotographs of the studied highly volatile bituminous coals from Greenland and Spitsbergen (non-polarised reflected white light, oil-immersion objective 50×). **a** Vitrodetrinite with fragmented fusinite, inertodetrinite, and sporinite in a coal sample from Greenland. **b** Collotelinite with some preserved cell morphology and vitrodetrinite with fragmented fusinite in a coal sample from Greenland. **c** Collotelinite with internal reflections (minerals, volcanic ash, micrinite, fine inertinitic detritus), and cutinite in a coal sample from Spitsbergen. **d** Collotelinite with internal reflections (minerals, volcanic ash, micrinite, fine inertinitic detritus) and well-preserved, unfragmented fusinite with a typical "Bogen-structure" in a coal sample from Spitsbergen

$C_{21\text{-}25}$ ~ 1.7; CPI $C_{23\text{-}33}$ ~ 1.3; Table 3). In the Greenland samples, long-chain *n*-alkanes were much more abundant than in the Spitsbergen coals, as reflected by higher terrigenous/aquatic ratios (TAR) (7.5–13.6 *vs*. 0.4–0.8, Table 3).

Acyclic isoprenoids

All coals contained the acyclic isoprenoid hydrocarbons 2,6,10-trimethyltridecane (TMTD), nor-pristane (2,6,10-trimethylpentadecane, nPr), pristane (2,6,10,14-tetramethylpentadecane, Pr), and phytane (2,6,10,14-tetramethylhexadecane, Ph). These compounds showed lower absolute concentrations in the Greenland samples (4–8 µg/g TOC) than in the Spitsbergen samples (15–41 µg/g TOC). Pr/Ph ratios varied between 5.1 and 8.0 (Table 3). Greenland coals revealed ten times higher Pr/*n*-C_{17} and Ph/*n*-C_{18} ratios (16.0–18.2 and 1.1–1.4, respectively) than Spitsbergen coals (1.2–1.6, 0.2; Table 3). For detailed results, see Table 3. For detailed concentrations, see Supplementary Table 2.

Iso- and *anteiso*-alkanes

Doublets of terminally branched 2-methyl- (iso-) and 3-methyl- (*anteiso*-) alkanes were observed in all samples, but coals from Greenland had much lower concentrations of these compounds than Spitsbergen coals (For detailed concentrations, see Supplementary Table 2). Their chain lengths covered similar ranges in Greenland (C_{17}–C_{29}) and Spitsbergen (C_{15}–C_{29}) coals. Relative abundances of *iso*-alkanes always were about twice as high as those of *anteiso*-alkanes.

Sesqui- and diterpenoids

Bicyclic sesquiterpenes were found in all coals studied and were identified according to their elution orders and mass

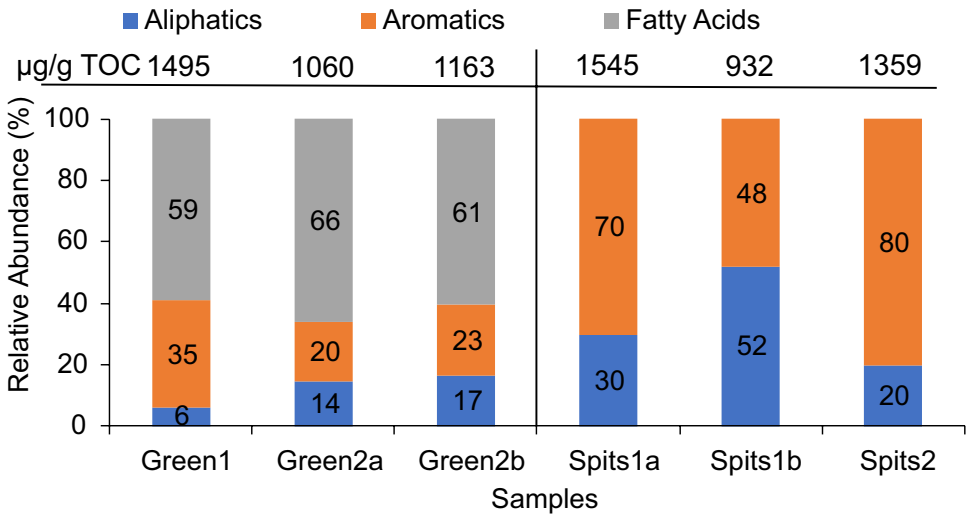

Fig. 4 Relative abundances of GC–MS amenable compound classes in the coal extracts (% of the TOEs). Numbers above the columns give the summed absolute concentrations (in µg/g TOC)

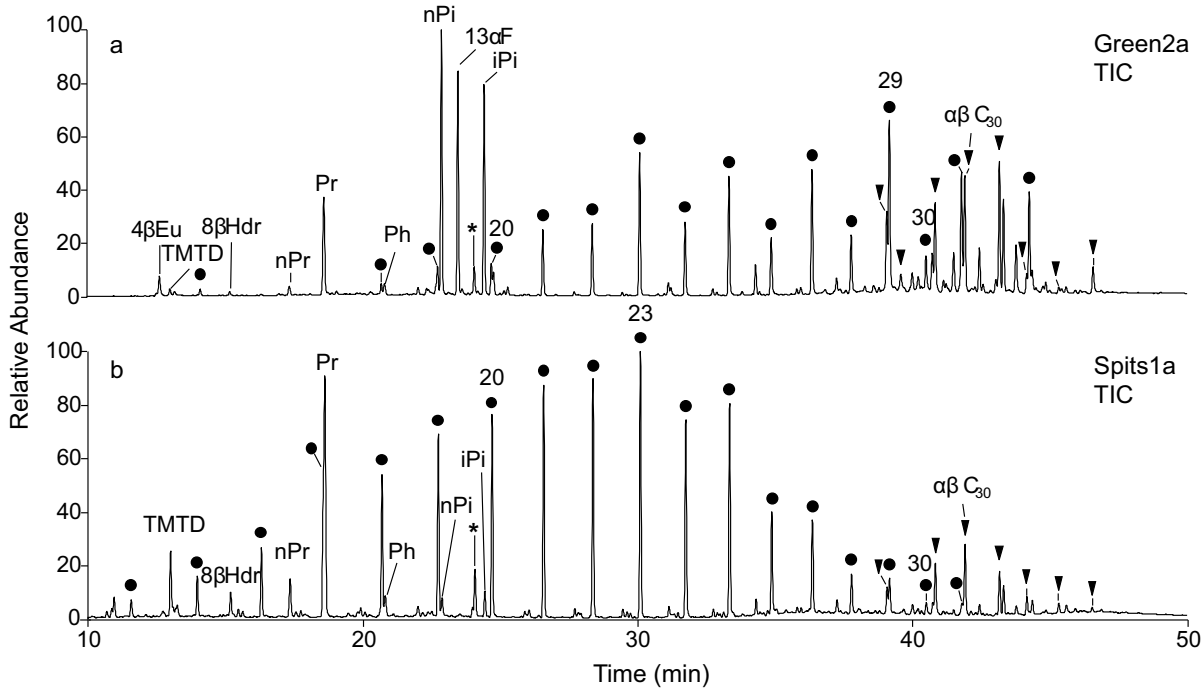

Fig. 5 GC–MS chromatograms (total ion current, TIC) of representative aliphatic hydrocarbon fractions (F1). **a** TIC of coal sample from Thyra Ø, Greenland. **b** TIC of coal sample from Longyearbyen Spitsbergen. Dots designate *n*-alkanes, numbers refer to carbon chain lengths. Triangles mark αβ-hopanes (22*S*-configuration for homohopanes); αβ C_{30} denotes 17α(H),21β(H)-hopane. *TMTD* 2,6,10-trimethyltridecane, *8βHdr* 8β(H)-homodrimane, *nPr* norpristane, *Pr* pristane, *Ph* phytane, *nPi* 4β(H)-19-norisopimarane, *iPi* isopimarane, *4βEu* 4β(H)-eudesmane, *13αF* 13α-fichtelite, *internal standard (*n*-icosane D_{42})

spectral fragmentation patterns (Alexander et al. 1983; Peters et al. 2005). 8β(H)-homodrimane was present at both sites, with the Greenland coals generally showing lower concentrations than Spitsbergen coals (Fig. 5; concentrations, see Supplementary Table 2). Low amounts of 8β(H)-drimane were found in Spitsbergen and not in the Greenland coals while 4α(H)- and 4β(H)-eudesmane occurrences are unique features of the Greenland coals. The abundance of 4β(H)-eudesmane in the latter, however, varied strongly, with 20

Table 3 Organic geochemical indices for aliphatic hydrocarbons

	Green1	Green2a	Green2b	Spits1a	Spits1b	Spits2
CPI[a] (C_{23-33})	3.0	2.8	1.8	1.4	1.3	1.2
OEP[b] (C_{15-19})	0.7	1.0	0.9	1.0	1.1	1.0
OEP[b] (C_{21-25})	3.1	2.8	2.4	1.8	1.8	1.7
ACL[c] (C_{27-31})	28.7	29.0	28.5	27.8	28.1	28.2
Pr/Ph[d]	6.8	6.7	5.1	8.0	5.4	5.5
Pr/*n*-C_{17}[e]	16.0	18.2	17.7	1.6	1.3	1.2
Ph/*n*-C_{18}[f]	1.1	1.2	1.4	0.2	0.2	0.2
TAR[g]	8.5	13.6	7.5	0.4	0.8	0.6
αββ-C_{29} $S/(S+R)$ steranes[h]	0.10	0.07	0.13	0.44	0.45	0.45
αββ-C_{29}/(αββ-C_{29} + ααα-C_{29}) steranes[i]	0.37	0.25	0.28	0.41	0.43	0.41
C_{29}/C_{27} steranes[j]	8.2	7.3	3.1	4.1	3.5	4.7
$C_{31}22S/(22S+22R)$ hopanes[k]	0.12	0.59	0.59	0.60	0.60	0.60
$C_{32}22S/(22S+22R)$ hopanes[k]	-	0.54	0.52	0.59	0.59	0.60
17α-hopanes/steranes[l]	8.9	10.2	5.0	16.6	12.1	16.5

[a]Carbon preference index (Bray and Evans 1961)

[b]Odd-even-predominance (Scalan and Smith 1970)

[c]Average chain length (Freeman and Pancost 2014)

[d]Pristane/phytane ratio (Didyk et al. 1978)

[e]Pristane/*n*-heptadecane ratio (Peters et al. 2005)

[f]Phytane/*n*-octadecane ratio (Peters et al. 2005)

[g]Terrigenous/aquatic ratio (Bourbonniere and Meyers 1996)

[h]$20S/(20S+20R)$ ratio of sterane epimers (Seifert and Michael Moldowan 1978)

[i]αββ-C_{29}/(αββ-C_{29} + ααα-C_{29}) ratio of steranes (Seifert and Michael Moldowan 1978)

[j]C_{29}/C_{27} Sterane ratio (after Huang and Meinschein 1979)

[k]$22S/(22S+22R)$ ratio of homohopanes (Ensminger et al. 1972)

[l]17α-hopanes/steranes (after Tissot and Welte 1984)

times higher concentrations in Green2b than in Green2a (both from the same Thyra Ø outcrop).

Tricyclic diterpenes were identified according to their mass spectral fragmentation patterns (key fragment: *m/z* 123) and elution orders according to Noble et al. (1985). Compound distributions are shown in Fig. 6. All samples contained isopimarane and/or 4β(H)-19-norisopimarane in high abundances (Supplementary Table 2). In Spitsbergen samples and Green1, isopimarane was the dominant diterpane (31–125 µg/g TOC), while coals from Thyra Ø (Green2a and Green2b) exhibited 4β(H)-19-norisopimarane not only as the main diterpane but even as the main compound of the aliphatic hydrocarbons (13–39 µg/g TOC). Small amounts of abietane were detected in all coals from Greenland, as well as in Spits1b and, in traces, in Spits2. In addition, 13-α(H)-fichtelite was observed in all Greenland samples, partly in relatively high concentrations (11 µg/g TOC in Green2b). Among the Spitsbergen coals, this compound occurred only in Spits2.

Tetracyclic diterpanes were identified according to their mass spectral fragmentation patterns (key fragments: *m/z* 259, 274) and elution orders after Noble et al. (1985). These compounds showed a greater variety and relative abundance within the Greenland than in the Spitsbergen coals (Supplementary Table 2). The Greenland sample from Fiskehalen (Green1) showed a predominance of *ent*-beyerane, followed by 16α(H)-phyllocladane and *ent*-16α(H)-kaurane. Small amounts of 16β(H)-phyllocladane and *ent*-16β(H)-kaurane occurred as well. The Greenland coals from Thyra Ø (Green2a and Green2b) revealed the highest concentrations of 16β(H)-phyllocladane. Except for *ent*-16α(H)-kaurane, the same tetracyclic diterpanes as in Green1 occurred in these samples, however in much lower concentrations. The Spitsbergen coals Spits2 and Spits1a showed only traces of *ent*-beyerane, 16β(H)-phyllocladane and *ent*-16β(H)-kaurane.

Steranes

Small quantities of C_{27}, C_{28} and C_{29} steranes were found in all coal samples (key fragments: *m/z* 217, 218) with C_{29} steranes as the dominant group. In the Greenland coal Green1 and in all Spitsbergen coals, the (20*R*)-5α(H),14β(H),17β(H)-isomer of 24-ethylcholestane

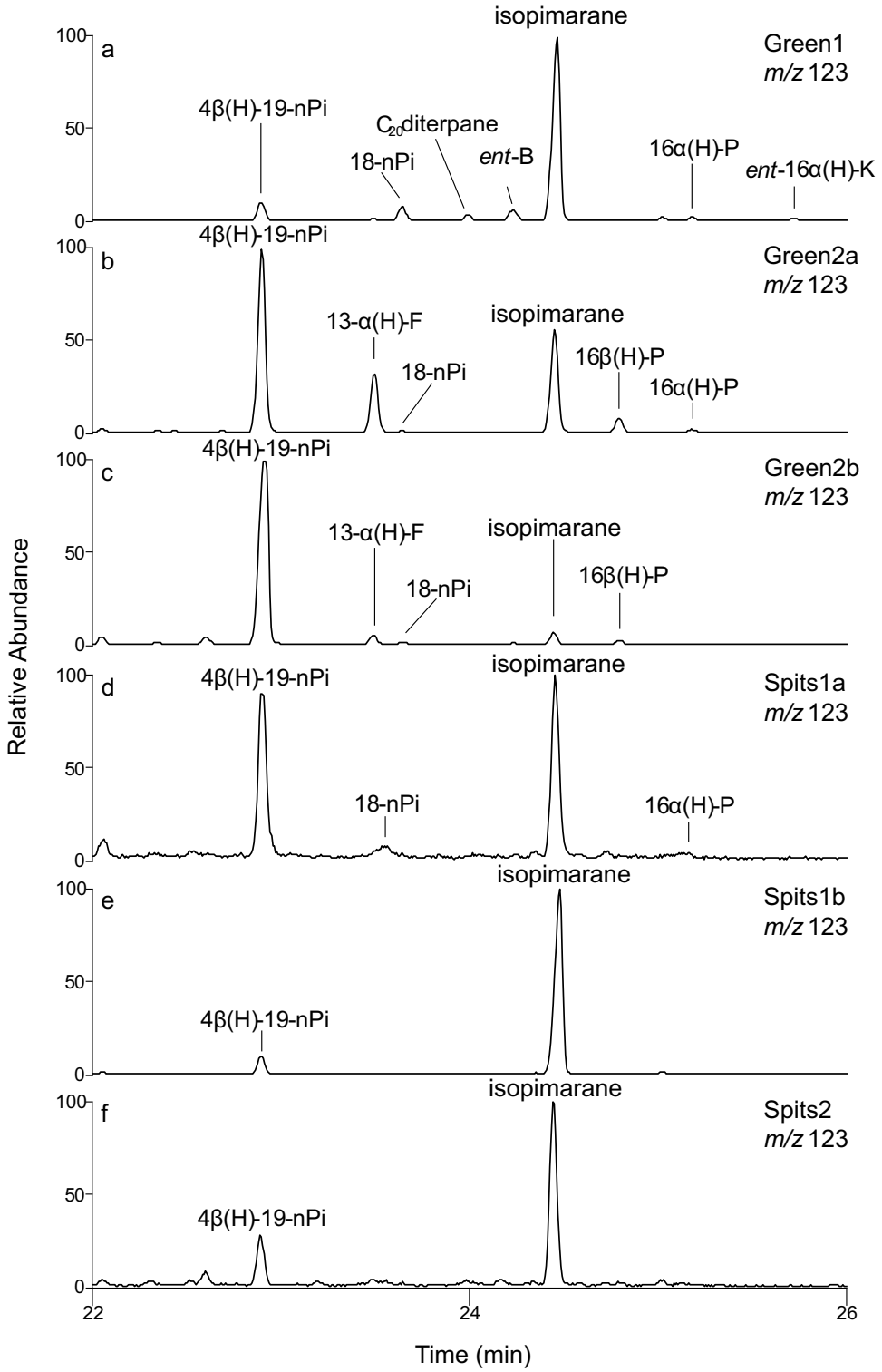

Fig. 6 GC–MS ion chromatograms (*m*/*z* 123) of aliphatic hydrocarbon fractions (F1) from Greenland and Spitsbergen coals, showing the distributions of tricyclic diterpenoids. **a**–**c** Ion chromatograms (*m*/*z* 123) from Greenland coals. **d**–**f** Ion chromatograms (*m*/*z* 123) from Spitsbergen coals. *4β(H)-19-nPi* 4β(H)-19-norisopimarane, *13-α-(H)-F* 13-α(H)-fichtelite, *18-nPi* 18-norpimarane, *ent-B* ent-beyerane, *16β(H)-P* 16β(H)-phyllocladane, *16α(H)-P* 16α(H)-phyllocladane, *ent*-16α(H)-K ent-6α(H)-kaurane

(αββ-C_{29} 20*R*) was the most abundant sterane, whereas ααα-C_{29} 20*R* was the dominant component in the Greenland coals Green2a and Green2b (for detailed concentrations, see Supplementary Table 2). Only traces of C_{27} and C_{28} steranes in different configurations were detected.

The 20*S*/(20*S* + 20*R*) ratios for ααα-C_{29} and αββ-C_{29} were consistent in samples from the same region (Table 3). The Greenland coals had lower values (~ 0.1) than those from Spitsbergen which were close to the geological equilibrium (~ 0.55). αββ-C_{29}/ (αββ-C_{29} + ααα-C_{29}) ratios show low and variable values (0.25–0.37) for Greenland coals while higher and more constant values (0.41–0.43) were observed for Spitsbergen coals (Table 3). C_{29}/C_{27} sterane ratios showed more variation in Greenland than in Spitsbergen samples (Table 3).

Pentacyclic triterpenoids

Traces of 17α(H)-22,29,30-trisnorhopane (identified after Philp 1985; Stout 1992), and two pentacyclic triterpenoids, tentatively identified as olean-12-ene and friedel-18-ene (Philp 1985), were detected in all coals. Green1 showed higher relative amounts of these components compared to all other samples (for detailed concentrations, see Supplementary Table 2). *Des*-A-lupane was observed as a minor compound in all samples except Green1 (identification after Philp 1985).

All coals showed unusually high amounts of hopanes (key fragment: *m/z* 191), with abundances ranging between 8 and 27% of the aliphatic hydrocarbon fractions. Carbon numbers typically ranged from C_{27} to C_{34}. 22*S*/(22*S* + 22*R*) stereoisomer ratios of 17α(H),21β(H)-homohopanes (αβ-hopanes) are listed in Table 3. In the Greenland coals from Thyra Ø (Green2a and Green2b) αβ-C_{30} and αβ-C_{31} were the most abundant hopanes, the latter showed 22*S*/(22*S* + 22*R*) ratios slightly above 0.5 and thus, a predominance of the geological 22*S*- over the biological 22*R* stereoisomer. In contrast, Green1 showed αβ-C_{31} in the biological 22*R*-configuration as the main hopanoid hydrocarbon. In this sample, only a small amount of the corresponding geological 22*S* stereoisomer was detected (22*S*/(22*S* + 22*R*) = 0.12, Table 3), and only traces of other 22*S* homohopanes occurred. Likewise, Green1 still contains homohopanes showing the immature biological 17β(H),21β(H)-configuration (ββ-hopanes). In comparison to the Greenland samples, coals from Spitsbergen revealed more homogenous hopanoid distributions; αβ-hopanes were the most abundant stereoisomers by far (maximum at αβ-C_{30}), ββ-hopanes were virtually absent, and all samples revealed 22*S*/(22*S* + 22*R*) ratios of 0.6, i.e. at the geological equilibrium (Table 3).

The hopane/sterane ratios for all coals studied were in a range from 5.0 to 16.6 and thus, remarkably high. Greenland samples revealed, however, lower values than Spitsbergen coals (Table 3).

Aromatic hydrocarbons

Alkylnaphthalenes

Alkylnaphthalenes were abundant in all samples (Fig. 7) and consisted of methyl-, dimethyl-, trimethyl- and tetramehtylnaphthalenes (MN, DMN, TMN, TeMN). Identification was based on mass spectral fragmentation patterns and elution orders shown in Rowland et al. (1984). TMNs represented over 50% of the total alkylnaphthalenes the coals from Thyra Ø (Green2a: 25 µg/g TOC,Green2b: 21 µg/g TOC) and the Spitsbergen coals from Longyearbyen (Spits1a: 246 µg/g TOC, Spits1b: 92 µg/g TOC). In these samples, either 1,2,7-TMN or 1,2,5-TMN occurred at the highest concentration in the aromatic fractions (each sample ~ 30–40% of the TMNs). In Spits2, 1,2,5,6-TeMN was the most abundant alkylnaphthalene (Greenland samples: 10–12 µg/g TOC, Spitsbergen samples: 23–66 µg/g TOC). For detailed concentrations, see Supplementary Table 3. The trimethylnaphthalene ratio (TNR) calculated after Alexander et al. (1985) was used to estimate the thermal maturity (Table 4). Hereon, the coals from Greenland showed lower values than the coals from Spitsbergen.

Phenanthrenes

Phenanthrene and its alkylated derivatives (methyl-, dimethyl-, trimethylphenanthrenes = MP, DMP, TMP) are present in all samples (Fig. 7, for detailed concentrations, see Supplementary Table 3). Peak identification was achieved according to elution orders (Radke et al. 1986) with respective key fragments *m/z* 178, 192, 206, 220. In Green2a, Green2b, Spits1b and Spits2 1,7-DMP showed the highest concentration of the triaromatic PAHs (Greenland, Thyra Ø: 8–10 µg/g TOC; Spitsbergen, Longyearbyen and Grumantbyen: 28–41 µg/g TOC), while Green1 and Spits1a had phenanthrene in highest amounts (9 and 18 µg/g TOC). TMP were present in all samples and accounted for 20 to 30% of triaromatic PAHs (Greenland: 5–11 µg/g TOC, Spitsbergen: 40–68 µg/g TOC). Calculated vitrinite reflectance values (%R_c, Radke et al. 1986) were determined from the methylphenanthrene index MPI-1 (using the methylphenanthrene ratio as an auxiliary parameter, Table 4). Coals from Greenland showed lower %R_c values than those from Spitsbergen (Table 2).

Aromatic sesqui- and diterpanes

Aromatic hydrocarbons derived from plant terpenoids were abundant in all coals (Fig. 7) and were identified using published mass spectra and elution orders (Ćmiel and Fabiańska 2004; Otto and Simoneit 2001; Philp 1985; Simoneit and

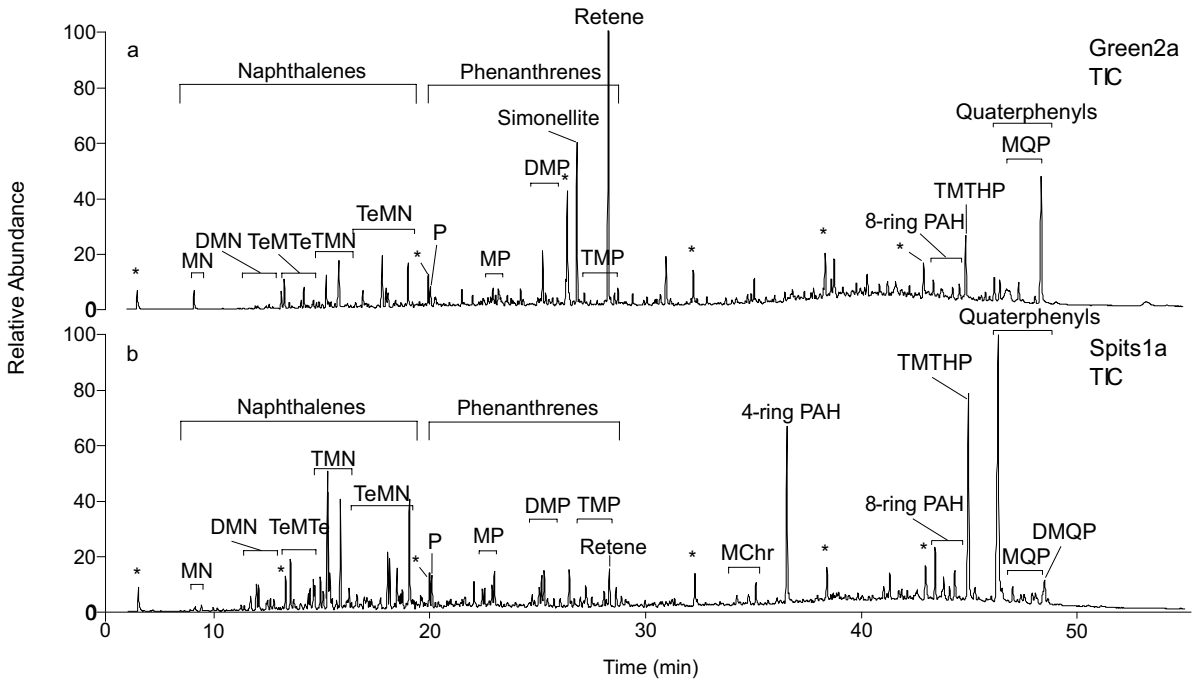

Fig. 7 GC–MS chromatograms (total ion current, TIC) of representative aromatic hydrocarbon fractions (F2). a TIC of coal sample from Thyra Ø, Greenland. b TIC of coal sample from Longyearbyen, Spitsbergen. 4-ring PAH unidentified polycyclic aromatic hydrocarbon, 8-ring PAH unidentified polycyclic aromatic hydrocarbon, MN methylnaphthalene, DMN dimethylnaphthalene, TeMTe tetrahydrotrimethylnaphthalene, TMN trimethylnaphthalene, TeMN tetramehtylnaphthalene, P phenanthrene, MP methylphenanthrene, DMP dimethylphenanthrene, TMP trimethylphenanthrene, MChr methylchrysene, TMTHP trimethylated 1,2,3,4 tetrahydropicenes, MQP methylquaterphenyl, DMQP dimethylquaterphenyl, *internal standard compounds

Table 4 Geochemical parameters for aromatic compounds

	Green1	Green2a	Green2b	Spits1a	Spits1b	Spits2
TNR-1[a]	0.2	0.3	0.4	0.5	0.5	0.9
MPR[b]	0.1	0.3	0.3	0.5	0.5	0.3
MPI-1[c]	0.10	0.33	0.31	0.55	0.54	0.37

[a]Trimethylnaphthalene ratio, (Alexander et al. 1985)

[b]Methylphenanthrene ratio, auxiliary parameters for 2c (Radke et al. 1986)

[c]Methylphenanthrene index, (Radke et al. 1986)

Mazurek 1982). In all samples, the aromatic sesquiterpanes cadina 1(10),6,8-triene, cuparene, and cadalene were detected (key fragments: *m*/*z* 187, 132, 183). Notably, the samples from Greenland exhibited a higher abundance of aromatic sesquiterpanes (9–30 µg/g TOC) compared to those from Spitsbergen (2–6 µg/g TOC). All coals featured high concentrations of retene (key fragment: *m*/*z* 219, 20–117 µg/g TOC), where Green1 and Spits2 had the highest quantities in this sample set. The aromatic diterpenoid simonellite (key fragment: *m*/*z* 237) was only detected in Greenland samples, despite low amounts. The monoaromatic diterpenoid dehydroabietane (key fragment: *m*/*z* 255) was present in Green1 and in traces in Green2b. 2-Methyl-1-(4-methylpentyl)-6-isopropylnaphthalene occurred in all samples except Spits1a.

Polycyclic aromatic hydrocarbons

The polycyclic aromatic hydrocarbons (PAHs) fluorene, dibenzofuran, and dibenzothiophene, with their respective alkylated derivatives, were tentatively identified in all samples in low concentrations after data given by Li et al. (2013). Three different methylpyrenes, two benzofluorenes ([*a*], [*b*]) and three methylfluoranthene derivatives were tentatively identified after Fang et al. (2015). Five-ring aromatic compounds were tentatively identified after Marynowski

et al. (2015) in all samples, with lower abundances in Greenland than in Spitsbergen samples. While all coals from Greenland contained perylene, Spits2 was the only sample from Spitsbergen in which it was detected. Minor contents of benzo[*b*]-fluoranthene, benzo[*k*]-fluoranthene, benzo[*i*]-fluoranthene, benzo[*a*]-fluoranthene, benzo[*e*]-pyrene and benzo[*a*]-pyrene were also detected in coals from both sites. For detailed concentrations, see Supplementary Table 3.

Higher molecular weight PAHs

Higher condensate PAHs were found in all coals (Fig. 7, for detailed concentrations, see Supplementary Table 3). Three not fully aromatised trimethylated 1,2,3,4-tetrahydropicenes (TMTHPs) were tentatively identified after Meyer et al. (2014) and Widodo et al. (2009). Except for Spits2, TMTHPs occurred in moderate to high concentrations in all coals. Especially in Green1 and Spits1, 2,2,9-TMTHP was very abundant (< 100 µg/g TOC). Also, Green1 showed high concentrations of isomer 1,2,9-TMTHP (46 µg/g TOC). The nine-ring PAH naphtho[8,1,2-*abc*]coronene was tentatively identified after Thiäner et al. (2019); three related compounds with the same mass ion but different retention times were detected. Further, a series of four peaks with a pronounced *m/z* 388 ion fragment was tentatively designated as a $C_{31}H_{16}$ nine-ring PAH after Thiäner et al. (2019). Given the possible presence of the aforementioned naphtho[8,1,2-*abc*]coronene, these peaks could represent methylated derivatives of these compounds. In addition, quarterphenyls and their methyl derivatives were tentatively identified after Marynowski et al. (2001) in all samples (Fig. 7). However, their distribution and concentration varied highly between the samples. Particularly high abundances of quarterphenyls were observed in Spits1a (177 µg/g TOC).

Fatty acids

n-Alkanoic acids

n-Alkanoic acids from C_{11} to C_{31} showing a strong even carbon number predominance were highly abundant in Greenland coals, whereas these compounds occurred only in minor amounts in Spitsbergen coals. The Greenland coals always showed a maximum at *n*-tetracosanoic acid (*n*-C_{24}), whereas the Spitsbergen samples showed a high relative abundance of *n*-C_{16} to *n*-C_{18} (Fig. 8). For detailed concentrations, see Supplementary Table 4.

In addition to *n*-alkanoic acids, doublets of *iso*- and *anteiso*-alkanoic acids were present as minor compounds in all coals from Greenland but were virtually absent in samples from Spitsbergen. If present, *iso*-isomers were always more abundant than *anteiso*-isomers. Furthermore, low amounts of phytanic acid were exclusively present in the Greenland samples.

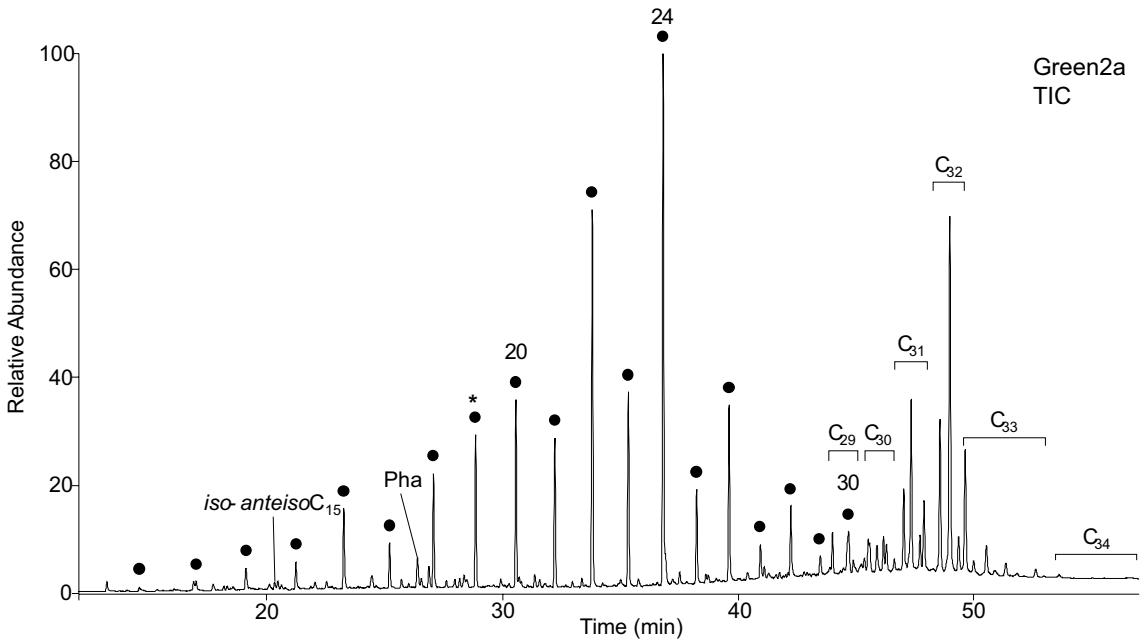

Fig. 8 GC–MS chromatogram (total ion current, TIC) of the carboxylic acid fraction (F3) obtained from a Greenland coal (Green2a). Dots designate *n*-alkanoic acids with numbers referring to their chain length. *internal standard. $C_{29\text{-}34}$ hopanoic acids with respective carbon chain length (brackets span the elution interval of different stereoisomers), *iso- anteiso*-C_{15} = *iso-* and *anteiso*-pentadecanoic acids, *Pha* phytanic acid

Hopanoic acids

Hopanoic acids (key fragment: *m*/*z* 191) with carbon numbers from C_{29} to C_{34} were detected only in the coals from Greenland (Fig. 8; for detailed concentrations, see Supplementary Table 4). In all these samples, αβ-C_{32} (22*R*) yielded the highest concentrations by far. Virtually all αβ- and βα- and ββ-stereoisomers were present in 22*S*- and 22*R* configuration, generally showing a preference for 22*R*-configuration. Additionally, the side chain carboxyl group creates a new chiral centre for C_{29} and C_{30} hopanoic acids, which enables 22*S*- and 22*R*-configuration; these stereoisomers were also observed in the samples. In Green2a and Green2b relatively high abundances of αβ-C_{31} (22*S*- and 22*R*-) hopanoic acids were also observed.

The quantitative distribution of hopanoic acids in samples from Fiskehalen (Green1) was different from the other Greenland coals sampled from Thyra Ø. Over 40% of the total hopanoic acids were ββ- stereoisomers (C_{29} to C_{34}), with ββ-C_{32} being the predominant pseudohomologue (92 µg/g TOC). Generally, concentrations of the αβ- and βα-hopanoids were smaller in Green1 than in Green2a and Green2b.

Discussion

Bulk geochemical and coal petrological similarities between Greenland and Svalbard coals

Palaeocene coals from Spitsbergen and Palaeogene coals from NE Greenland have OI values (or O/C ratios) lower than those of typical type III kerogen coals (Peters 1986; van Krevelen 1993), suggesting a specific and similar type of source vegetation or diagenetic transformation pathway.

All examined coals have relatively high HI values in common (mostly between 300 and 400 mg hydrocarbons/g TOC), which is often associated with sapropelic coals and high amounts of liptinite ("oil-prone"). All studied coals, however, are humic coals with low abundances of liptinite (Table 2). Reasons for the relatively high HI values of the vitrinite-rich coals from Spitsbergen have been previously discussed (Orheim et al. 2007), but the controls are still not well understood. Potential factors are a high bacterial reworking combined with marine influence and/or the specific temperate high latitude setting at the time of deposition (Marshall et al. 2015a). For the studied Greenland coals, our data are novel and demonstrate similar geochemical compositions to the coals of Spitsbergen and likely a comparable formation pathway and palaeoenvironment (see detailed discussion below).

The maceral group analyses revealed a similarity among the examined coals displaying a dominant content of the vitrinite maceral group, followed by a roughly comparable content of liptinite and inertinite maceral groups. However, within both the Greenland and Spitsbergen coals, different macerals of vitrinite maceral group predominate in the maceral assemblage. The higher contents of the detrovitrinite subgroup in the Greenland coals demonstrate a relatively higher degree of comminution from parenchymatous and woody tissues. Such a high degree of fragmentation implies an alteration in cell mechanical properties as well as in the water content of the cell tissues, possibly during enzyme hydrolysis initiated by microbial decay. Higher telovitrinite subgroup contents, occurring in Spitsbergen coals suggest that conditions for peat preservation were particularly favourable. The preservation of telovitrinite is generally improved by anoxic conditions, which inhibits the oxidation of peat. It can be inferred that the water table of the palaeomire was relatively high during its growth and development.

Coalification (maturity)

Vitrinite reflectance measurements showed that the coal rank of the Greenland Thyra Ø coal (Green2b) is the lowest in the examined sample set (high volatile bituminous coal rank with 0.49% VRr). Similarly low is the rank of the Greenland coal Green1 (0.53% VRr) and the degree of coalification of Green2a was observed to be slightly higher (0.59% VRr). The Spitsbergen coals show the relatively highest ranks in our data set (high volatile bituminous coal rank with VRr of 0.68–0.75%). Our data for the coals from Thyra Ø (Green2a and Green2b) are in line with published values from the same area (Paech and Estrada 2019). T_{max} values from Rock–Eval support the relative order of studied samples in terms of thermal maturity (Table 2, Fig. 9). The bulk organic geochemistry for Palaeocene coals from Spitsbergen and the coalification derived thereof are in good agreement with previous reports (Marshall et al. 2015a).

Additional support for the differences in coalification degree comes from aliphatic and aromatic biomarker parameters. CPI and OEP typically decrease in the course of thermal maturation, with values around unity being reached upon entry into the oil window (Marzi et al. 1993; Peters et al. 2005; Scalan and Smith 1970). All coals studied still exhibit a preference for *n*-alkanes with odd carbon chain lengths, but values of CPI and OEP in the Greenland samples are significantly higher than in Spitsbergen samples (Table 3). This supports Vitrinite reflectance data of a somewhat lower maturity of the coals of Greenland compared to those of Spitsbergen.

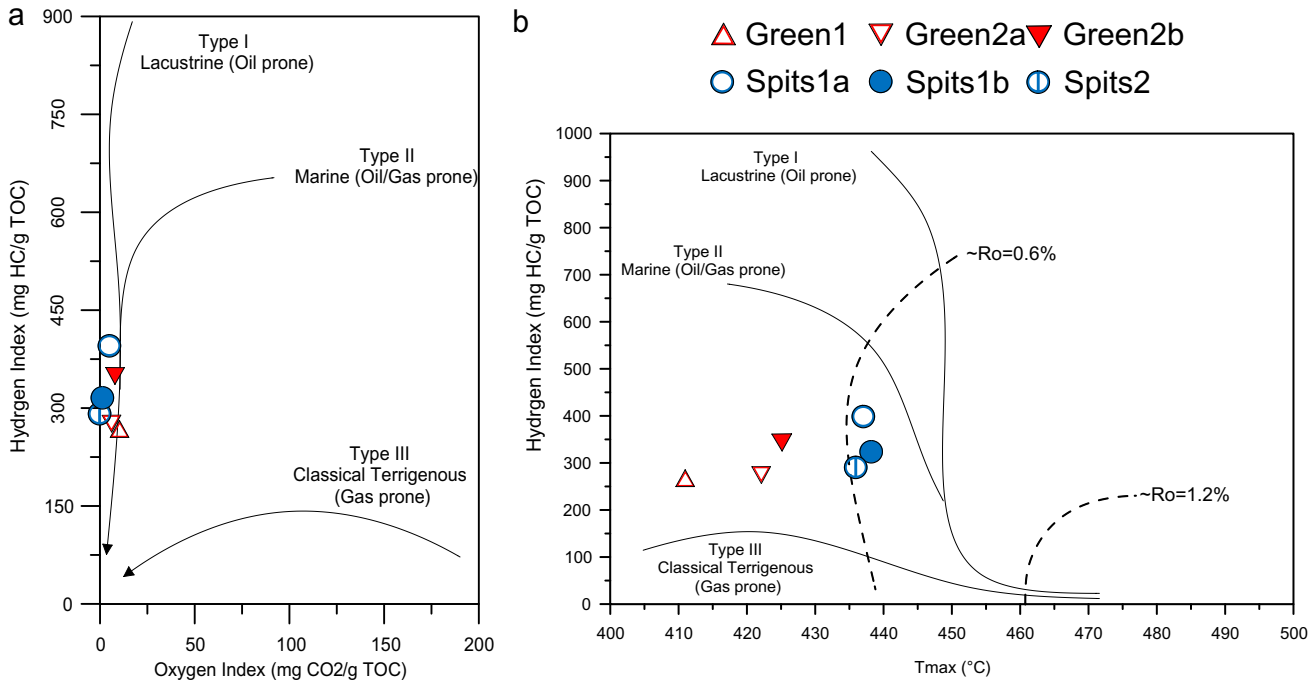

Fig. 9 Rock–Eval data of coals from Greenland and Spitsbergen. **a** Pseudo-van Krevelen diagram. **b** Hydrogen index (HI) vs. T_{max} (maturity) plot

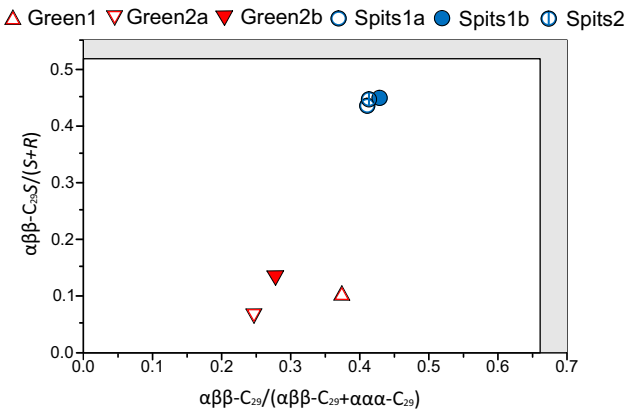

Fig. 10 Correlation of sterane αββ-C_{29} $S/(S+R)$ and αββ-C_{29}/(αββ-C_{29} + ααα-C_{29}) isomer ratio reflecting thermal maturity (Peters et al. 2005). Grey area marks reaction endpoint

Likewise, homohopane isomer ratios $22S/(22S+22R)$ (Ensminger et al. 1972; Peters et al. 2005) of most samples are at, or close to, equilibrium (0.6), which is typically reached at the beginning of the oil window (Table 3). Only the sample from the Greenland Fiskehalen outcrop (Green1) showed an exceptionally low value (0.12), in line with a relatively low maturity. Supportive for the maturity order of the studied samples are also the sterane isomer ratios (αββ-C_{29} $S/(S+R)$ and αββ-C_{29}/(αββ-C_{29} + ααα -C_{29}) (Peters et al. 2005, Fig. 10, Table 3). Spitsbergen coals are close to the reaction equilibrium, which is associated with the onset of oil generation at 0.7 Rr% (Marshall et al. 2015b; Peters et al. 2005). Similar values for the Spitsbergen coals were reported by Marshall et al. (2015b).

Among the aromatic compounds the TNR (Alexander et al. 1985; Peters et al. 2005) and MPI-1 (Peters et al. 2005; Radke et al. 1986) indices obtained from isomer patterns of naphthalenes and phenanthrenes, respectively, support the findings from the aliphatic fractions, showing lower thermal maturity of Greenland than Spitsbergen samples (see Table 3, Table 4).

In addition to these indices, it should also be considered that the overall degree of aromatization reflects the advance of coalification. Less mature samples contain a higher concentration of partially aromatised compounds as compared to more mature samples which show a higher proportion of fully aromatised structures (Fabiańska and Kurkiewicz 2013). The coals from the Greenland Thyra Ø outcrop (Green2a and b) have much higher concentrations of simonellite than the Greenland coal from Fiskehalen (Green1).

Spitsbergen coals, in contrast, are dominated by fully aromatised compounds. Especially retene is abundant, accompanied by only small amounts of simonellite (Fig. 7).

Palaeovegetation in the coal swamps

The Palaeogene age of the sediments in NE Greenland and Spitzbergen has been derived from palynological investigations, e.g. Lyck and Stemmerik (2000) and Manum and Throndsen (1986) respectively. Boyd (1990, 1992) has described the palaeovegetation of the Thyra Ø Formation based on macrofossil findings, mainly leaves. O. Heer documented such fossils from the Van Mijenfjorden Group in Spitsbergen already in the late nineteenth century (see Boyd 2000 for references). Both floras contain abundant angiosperms and gymnosperms like *Metasequoia*, interpreted to reflect warm climate conditions in the northern high latitudes during the Palaeogene.

A considerable amount of the detected organic compounds in our coal samples are sourced by higher plants. Table 5 provides an overview of selected components and their possible biological origins.

The studied coals from Spitsbergen and Greenland contain *n*-alkanes between *n*-C_{27}-*n*-C_{33}, implying the presence of higher plants (Otto et al. 2005). In particular, the long chain length *n*-alkanes exhibit a predominance of odd chain lengths, while at shorter *n*-alkanes neither odd nor even chain lengths dominate (OEP, Table 3). Coals from both studied regions contain comparable relative proportions of mid-range *n*-alkanes (*n*-C_{21} to *n*-C_{25}), which are an indicator for sphagnum (peat ferns), lichens and/or aquatic macrophytes (Baas et al. 2000; Ficken et al. 2000; Nott et al. 2000). Their occurrence in the Palaeogene Arctic swamps is very likely and further implied by the second maximum within this range of *n*-C_{23} or *n*-C_{25} of the samples from Greenland (Fig. 5a). These differences in the relative abundance of *n*-alkane distribution between coals from Greenland and Spitsbergen are likely related to their differing coalification. Assuming this mechanism, Greenland coals can be interpreted as reflecting the closer initial distribution of *n*-alkanes. Regarding the proximity of Spitsbergen to Greenland during the Palaeogene, a similar ecosystem with comparable vegetation is likely. While the short-range *n*-alkanes (*n*-C_{14}-*n*-C_{20}) can also be a product of thermal maturity, it is unlikely to show a preference of a chain length at the same time. Likewise, to the *n*-alkanes, the alkanoic acids in Greenland show a typical distribution for higher plants with a dominance of longer and even carbon chains (Eglinton and Murphy 1969; Freeman and Pancost 2014; Logan et al. 1995). Conceivably, the lack of alkanoic acids in the coals from Spitsbergen is attributed to their higher maturity. The dominance of *iso*- and *anteiso*-alkanes with longer and even carbon chain lengths is another indication for the presence of higher plants in the Greenland and Spitsbergen coals (Freeman and Pancost 2014; Tissot and Welte 1984). All coals show the highest amounts of C_{29} steranes, which are mainly derived from higher plants (Huang and Meinschein 1979; Izart et al. 2015; Philp 1985; Fig. 11; Table 3). In addition to the plant-derived stigmastane C_{29} steranes can also be produced by fucosterol, which is produced by brown algae (Killops and Killops 2004), but due to the general predominance of terrestrial biomarkers, a marine influence was likely minor.

The presence of sesquiterpanes in all studied coals are another indicator of the strong higher plant input (Simoneit et al. 1986). Especially 4β(H)-eudesmane, which was only found in the coals from Thyra Ø (Green2a and Green2b), has a clear structural relation to the higher plant terpenes (Alexander et al. 1983; Peters et al. 2005). It is assumed, that their exclusive presence in these coals could indeed reflect a local source-specific origin of a yet unknown (higher) plant. They also observed drimanes miss the clear structural relation to specific compounds in plants and have furthermore, another biological source in prokaryotes (Alexander et al. 1984; Peters et al. 2005). Within this sample set, higher total concentrations of drimanes coincide with higher total concentrations of hopanoids making a mostly prokaryotic origin likely. Aromatic sesquiterpenoids are commonly used as markers for higher terrestrial plants because they occur in resinous material in both, gymnosperms and angiosperms (Haberer et al. 2006 and references therein). Cadalene is ubiquitous in higher plants (Bordoloi et al. 1989; Peters et al. 2005), although a marine origin is possible (van Aarssen et al. 2000). The occurrence of cadalene and related compounds in coals serves also as an indicator of higher plant input. Cadina-1(10),6,8-triene, cuparene and cadalene were observed in all samples and underline the close relationship between the samples and the prevalence of terrigenous plant biomarkers. Moreover, cadalene can be specific for the angiosperm's family *Dipterocarpaceae*. This plant family is today typically found in modern rainfed lowland peat swamps of tropical Indonesia (Widodo et al. 2009). A great variety and abundance of aliphatic and aromatic tricyclic diterpanes were found in the coals (Table 5). In general, these

Table 5 Overview of compounds detected in the coals from Spitsbergen and Greenland with their indication for different plants according to the references

Nr	Type	Compound	Possible Sources	Specifics	References
Alkanes					
1	Aliphatic	n-C_{20}-n-C_{29}	M, L, Pf		Baas et al. (2000), Ficken et al. (2000)
2	Aliphatic	> n-C_{29}	unsp. HP		Otto et al. (2005), Schlanser et al. (2020)
Alkylnaphthalene					
3	Aromatic	1,2,7- TMN	A		Chaffee and Johns (1983), Strachan et al. (1988)
Sesquiterpenoids					
4	Aliphatic	4α(H)-Eudesmane	unsp. HP		Alexander et al. (1983)
5*	Aliphatic	4β(H)-Eudesmane	unsp. HP		Alexander et al. (1983)
6*	aromatic	Cuparene	unsp. HP		Otto and Simoneit (2001)
7*	aromatic	Cadalene	unsp. HP		Otto and Simoneit (2001)
9*	aromatic	Cadina-1(10),6,8-triene	unsp. HP		Otto and Simoneit (2001)
Diterpenoids					
9	Aliphatic	C_{19} Norpimarane	G		Noble et al. (1986)
10*	Aliphatic	4β(H)-19 Norisopimarane	G		Noble et al. (1986)
11*	Aliphatic	13α(H)-Fichtelite	G	*Pi*	Otto and Simoneit (2001)
12	Aliphatic	C20 Diterpane	G		Philp (1985)
13*	Aliphatic	ent-Beyerane	G		Noble et al. (1985)
14*	Aliphatic	16β(H)-Phyllocladane	G	*Po*, *Ar*, *Cu*	Noble et al. (1985)
15*	Aliphatic	*ent*-16β(H)-Kaurane	G	*Po*, *Ar*, *Cu*	Noble et al. (1985)
16	Aliphatic	16α(H)-Phyllocladane	G	*Po*, *Ar*, *Cu*	Noble et al. (1985)
17	Aliphatic	*ent*-16α(H)-Kaurane	G	*Po*, *Ar*, *Cu*	Noble et al. (1985)
18	Aliphatic	18-NorIsopimarane	G		Noble et al. (1986)
19*	Aliphatic	Abietane	G		Otto and Wilde (2001)
20*	Aliphatic	Isopimarane	G		Otto and Wilde (2001)
21	Aliphatic	4α-(H)-18-Norisopimarane	G		Noble et al. (1986)
22*	Aromatic	Dehydroabietane	G		Otto and Simoneit (2001)
23*	Aromatic	Simonellite	G		Otto and Simoneit (2001)
24*	Aromatic	Retene	G		Otto and Simoneit (2001)
Triterpenoids					
25*	Aliphatic	*des*-A-Lupane	A		Otto and Simoneit (2001)
26*	Aliphatic	Olean-12-ene	A		Otto and Simoneit (2001)
27*	Aliphatic	Friedel-18-ene	A		Otto and Simoneit (2001)
28	Aromatic	1,2,9-TM-1,2,3,4-tetrahydropicene	A		Widodo et al. (2009)
29	Aromatic	2,2,9-TM-1,2,3,4-tetrahydro-picene	A		Widodo et al. (2009)

M, *L*, *Pf* macrophytes, lichens and peat ferns, unsp; *HP* unspecified higher plants, *G* gymnospermes with conifers, *A* angiosperms, *TMN* trimethylnaphthalene, *TM* trimethyl, *Pi Pinus palaeostrobus Po*, *Ar*, *Cu Podocarpaceae*, *Araucariaceae*, *Cupressacea.* *for structures see appendix Fig. 13

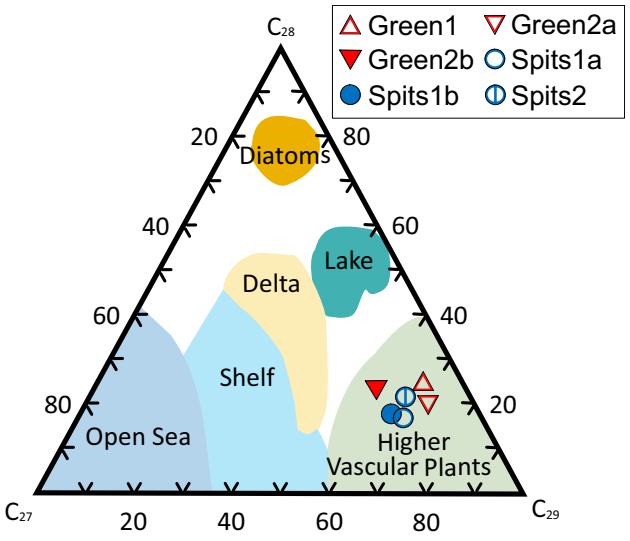

Fig. 11 Ternary diagram of $C_{27,}$ C_{28} and C_{29} steranes, indicating primary organic matter source and depositional environment (modified after Fabiańska and Kurkiewicz 2013, based on Huang and Meinschein 1979)

components are considered unspecific conifer biomarkers (Otto and Wilde 2001; Schlanser et al. 2020), because high concentrations of diterpane-precursors are found in many conifer resins (Otto and Simoneit 2001; Simoneit 1977 and references therein). Some tricyclic diterpanes can even be indicative for specific families within the conifers: for example, 13α(H)-fichtelite is a major compound in *Pinus palaeostrobus* (Otto and Simoneit 2001), which was found in coals from both regions, Greenland and Spitsbergen. All tetracyclic diterpanes found in the studied coals are thought to have precursors in leaf resins of conifers, possibly from the *Podocarpaceae*, *Araucariaceae*, and *Cupressaceae* families (Noble et al. 1985; Peters et al. 2005). Although *Podocarpaceae* and *Araucariaceae* are currently restricted to the southern hemisphere in tropical areas, geochemical and palaeobotanical studies show evidence of these pine species in the higher northern hemisphere during the Palaeogene (Ćmiel and Fabiańska 2004; Poinar et al. 1999,). Schlanser et al. (2020) note the rarity of *Podocarpaceae* and *Araucariaceae* in the Palaeogene and consider the *Cupressaceae* family as the most suitable origin as it is also induced by the macro fossils in Dolezych et al. (2019).

Pentacyclic terpenoids of the oleanane, ursane, lupane and friedelin classes are almost exclusively produced by angiosperms and are parts of their leaf waxes (Freeman and Pancost 2014; Otto and Simoneit 2001). Oleananoids, lupanoids and friedelanoids are present in the studied coals, as well as the diagenetic product TMTHPs (Table 5), proving a contribution of angiosperms to the coal-forming vegetation. Also, Angiosperm-derived are the observed partly aromatised picenes, which possibly originate from alpha- and beta-amyrin (Wakeham and Canuel 2016; Widodo et al. 2009).

Depositional environment and preservation

Different biomarkers are valid parameters for the depositional and redox environment. For instance, the pristane/phytane (Pr/Ph) ratio gives information about the redox conditions after organic matter deposition (Didyk et al. 1978). In anoxic environments, Pr/Ph ratios are below 1, alternating anoxic and oxic conditions are indicated by Pr/Ph ratios around 1. Pr/Ph ratios larger than 3 indicate terrigenous plant input deposited under oxic to suboxic conditions (Peters et al. 2005). By oxidation of the phytol side chain of chlorophyll, Pr is released, while reduction of the phytol side chain releases commonly Ph. However, numerous influences on the Pr/Ph ratio are known (Haven et al. 1987; Peters et al. 2005; Tissot and Welte 1984). The most relevant alternative source for pristane other than the oxic turnover of chlorophyll is tocopherol, a vitamin naturally occurring in higher plants or algae (Goossens et al. 1984). Nevertheless, all studied coals have similar Pr/Ph ratios > 5, indicating an oxic terrigenous deposition environment (Table 3). Variations in the Pr/Ph ratios can be attributed to fluctuating environmental conditions (groundwater level, rainwater, eustatic sea level) regulating the water balance and therefore the Eh and pH values at the sites (Bechtel et al. 2005). Similar Pr/Ph values to those found here for Spitsbergen coals were observed by Marshall et al. (2015b). Pr/*n*-C_{17} and Ph/*n*-C_{18} give further evidence of the depositional environment (Peters et al. 2005). *n*-C_{17} and *n*-C_{18} are influenced by maturity as well as biodegradation and water washing. All studied coals plot within or zone typical for deposition in peat swamps under oxic conditions (Fig. 12). Different positions of the coals from Greenland and Spitsbergen are likely a result of thermal maturation: through the cracking of longer *n*-alkanes, the amount of *n*-C_{17} and *n*-C_{18} will be increased. Consequently, the more mature Spitsbergen coals shift to the origin of the coordinate system.

The terrigenous/aquatic ratio (TAR) expresses the influence of terrestrial to aquatic inputs (Bourbonniere and Meyers 1996; Peters et al. 2005). Short chains *n*-alkane are indicators for marine algae and phytoplankton, while long

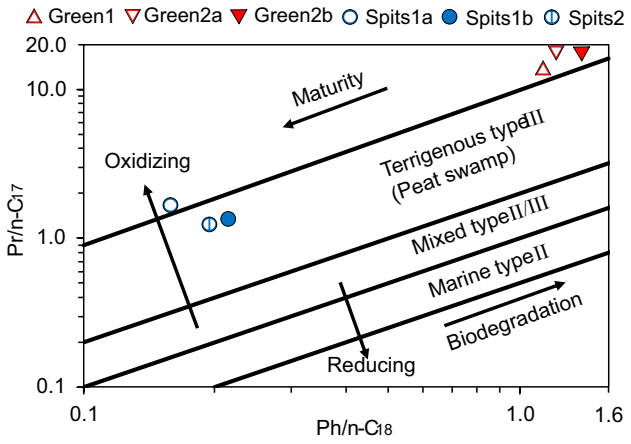

Fig. 12 Plot of Pr/*n*-C_{17} and Ph/*n*-C_{18} ratios indicative for different types of depositional environments (Peters et al. 2005). Different positions of coals from Greenland (red triangles) and Spitsbergen (blue circles) reflect higher maturity of Spitsbergen coals. Note double logarithmic axis

n-alkane chains can be traced back to the synthesis of land plants.

The TAR was calculated to visualise possible marine influences at the sites. However, an unexpected high difference between coals from Greenland (7.5–13.6, Table 3) and Spitsbergen (0.4–0.8, Table 3) was observed. However, the low TAR for Spitsbergen coals could be best explained by relatively high coalification. Through thermal stress, the relative proportion of short-chain *n*-alkanes increased by cracking of long-chain *n*-alkanes. Even though the TAR does not imply marine influence, there are clear signs of episodic marine ingressions on both investigated sites. Sedimentological and palynological data (Håkansson et al. 1991; Jochmann et al. 2020; Lyck and Stemmerik 2000) show typical facies indicating marginal marine influences during the Palaeogene in both basins. Moreover, relatively high concentrations of bulk sulphur within the coals (Table 2) imply a direct marine influence on the coal swamps. The TAR may not reflect this, as the relative proportion of marine biomarkers at the sites is subordinate compared to the overwhelming amount of terrestrial markers.

In the Palaeogene Arctic ecosystem, wildfires have likely played an important role (Denis et al. 2017). Consequently, wildfires should be seen as a possible source for some biomarkers, especially aromatics (Marynowski and Simoneit 2009; Marynowski et al. 2015; Otto et al. 2006; Thiäner et al. 2019; Wakeham and Canuel 2016 and references therein). Indeed, Marshall (2013) found weak evidence of wildfires within the coals from Longyearbyen in Spitsbergen. Hints for combustion within this study are low molecular weight PAHs like benzo[a]pyrene and pyrene, and high molecular weight PAHs like naphtho[8,1,2-*abc*]coronene (Denis et al. 2012; Thiäner et al. 2019). However, the inertinite proportion was less than 10% in all coals and the coals did not exhibit typical biomarker distributions for post-fire soils after Otto et al. (2006). Therefore, the influence of wildfires on the biomarker composition and, thus, the studied settings is regarded as outside conceptual model of deposition.

Bacterial input

The coals from Greenland and Spitsbergen contain high concentrations of hopanoids. Together with high 17α-hopanes/steranes ratios, this is evidence for high levels of bacterial reworking of organic matter in the palaeo-coal swamps (Ourisson et al. 1979, 1984; Volkman 2005). In all coals, high concentrations of 8β(H)-homodrimane (as well as related compounds from the drimane-series) and short *iso*- and *anteiso*-alkanes with respective fatty acids may be an additional record of high bacterial reworking (Alexander et al. 1984; Blumenberg et al. 2018; Killops and Killops 2004; Parkes and Taylor 1983). High values of hopanoids linked to bacterial activity in the Arctic Palaeogene environments are also reported by Ćmiel and Fabiańska (2004), Marshall et al. (2015a) and Schlanser K., pers. com.

The specific environment of the Arctic palaeo-swamps, recorded in the studied coals, could provide a possible explanation for the high occurrence of bacteria during deposition: throughout the Palaeogene, the likely connected coal swamp depositional environments of Greenland and Spitsbergen were at a similar latitude as today, facing several months of complete darkness during winter and conversely long periods of permanent daylight during summer. However, temperatures were high enough to provide suitable conditions for the formation of a peat swamp. We speculate that due to a more hostile environment for life compared to lower latitudes, the periods of complete darkness could

hamper light-dependent organisms (e.g., higher plants, algae). Thus, non-light dependent (e.g., decomposing) bacteria could have had long-lasting phases of relatively high productivity due to low ecological pressure from other organisms. The corresponding longer daylight periods in summer could, on the other hand, contributed to relatively high plant primary productivity (Konrad et al. 2023) which in turn could have served as the main carbon and energy source for the bacteria.

Conclusions

Geochemical and coal petrological data indicate that the coals from Greenland are less coalified compared to those from Spitsbergen. Among the Greenland coals, those from Thyra Ø Island showed a slightly higher degree of coalification (~ 0.5–0.6% VRr), while the sample from Fiskehalen displayed the lowest coal rank (~ 0.5% VRr) and additionally revealed exclusive biomarkers typical for very low maturity. Spitsbergen coals from Longyearbyen and Grumantbyen showed higher vitrinite reflectances (~ 0.6–0.75% VRr) and higher biomarker maturities.

The palaeo-vegetation showed a predominance of higher plants. Occurrences and distributions of distinctive plant-derived terpenoids reflect organic matter inputs from conifers and angiosperms. In addition, the high relative proportion of mid-range *n*-alkanes found in all coals suggests contributions from aquatic macrophytes.

The interpretation of the depositional environment, based on organic geochemistry, implies fluvio-deltaic environments and deposition under oxic conditions. Further, marginal marine influences are indicated by generally high sulphur contents of the coal samples. Wildfires are common phenomena in coal swamps, and their occurrence in the environments studied is reflected by the presence of abundant heavy PAHs.

Overall, the studied coals from Greenland and Spitsbergen share important geochemical and coal petrological similarities, whereas differences can, partly at least, be attributed to different thermal maturities (isomers ratios for hopanes and steranes, *n*-alkane distributions, and presence of fatty acids). Hence, our data are in good agreement with a widespread and connected coal swamp depositional setting between NE Greenland and Svalbard. Moreover, time-equivalent and comparable types of hydrogen-rich coals were also described from other regions in the Arctic (and from the southern hemisphere). Organic matter deposition in these extensive high-latitude coal swamps likely played a prominent role in atmospheric carbon drawdown during the high CO_2 phase of the Palaeogene.

Appendix

See Fig. 13.

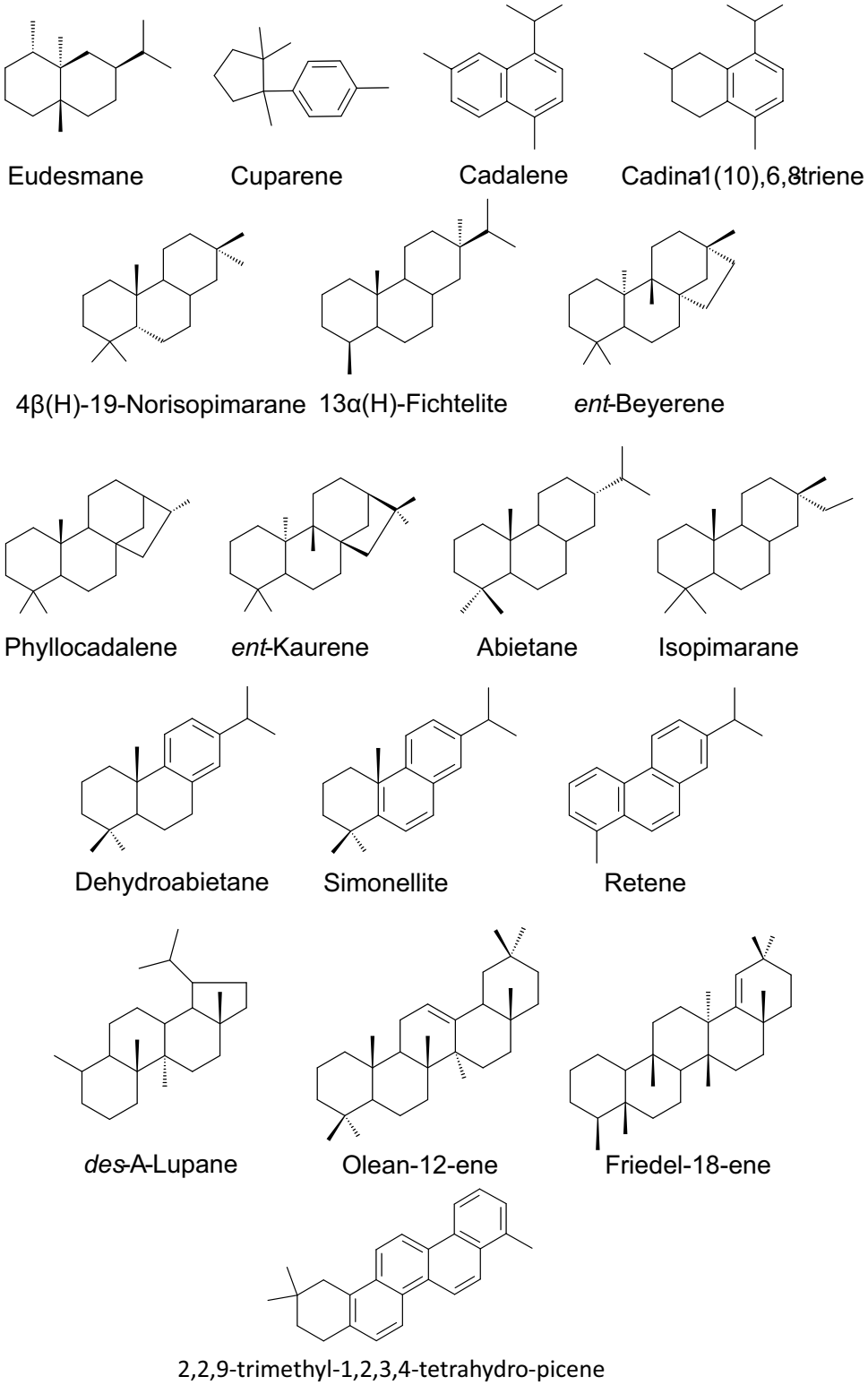

Fig. 13 Chemical structures cited

Supplementary Information The online version contains supplementary material available at https://doi.org/10.1007/s00531-024-02428-4.

Acknowledgements We acknowledge support by BGR's Arctic research project „Circum-Arctic Structural Events" (CASE) during expeditions CASE 17-2 (Svalbard) and CASE 20 (NE Greenland) organised by Karsten Piepjohn, enabling access to these remote outcrops. We thank Malte Jochmann (Longyearbyen) who made access to coal mine Gruve 7 possible. Many thanks to the staff and administration of the Villum Research Station operated by the University of Aarhus at the military outpost Station Nord (Kronprins Christian Land, NE Greenland). We are very thankful to the reviewers Achim Bechtel and Ksenija Stojanović for their helpful comments and suggestions. Sylvia Kramer, Yannick Meve, Mechthild Rittmeier, Birgit Röring, Ina Sosnitza, and Monika Weiß are thanked for their assistance during the laboratory work at the University of Göttingen and the BGR. Georg Scheeder and Petra Adam (both BGR) are thanked for their work in acquiring the Rock-Eval data. Philipp Weniger (BGR) and Kristen Schlanser (Wisconsin State Laboratory) are thanked for their input during the discussion of coal geochemistry and terpenoid preservation in this work.

Funding Open Access funding enabled and organized by Projekt DEAL.

Data availability Data are included in supplementary data.

Declarations

Conflict of interest The authors declare that they have no competing interests related to the research presented in this manuscript.

References

Alexander R, Kagi R, Noble R (1983) Identification of the bicyclic sesquiterpenes drimane and eudesmane in petroleum. J. Chem. Soc Chem Commun 5:226–228. https://doi.org/10.1039/c39830000226

Alexander R, Kagi RI, Noble R, Volkman JK (1984) Identification of some bicyclic alkanes in petroleum. Org Geochem 6:63–72. https://doi.org/10.1016/0146-6380(84)90027-5

Alexander R, Kagi R, Rowland S, Sheppard P, Chirila T (1985) The effects of thermal maturity on distributions of dimethylnaphthalenes and trimethylnaphthalenes in some Ancient sediments and petroleums. Geochim Cosmochim Acta 49(2):385–395. https://doi.org/10.1016/0016-7037(85)90031-6

Baas M, Pancost R, van Geel B, Sinninghe Damsté JS (2000) A comparative study of lipids in Sphagnum species. Org Geochem 31(6):535–541. https://doi.org/10.1016/S0146-6380(00)00037-1

Bechtel A, Sachsenhofer RF, Zdravkov A, Kostova I, Gratzer R (2005) Influence of floral assemblage, facies and diagenesis on petrography and organic geochemistry of the Eocene Bourgas coal and the Miocene Maritza-East lignite (Bulgaria). Org Geochem 36(11):1498–1522. https://doi.org/10.1016/j.orggeochem.2005.07.003

BGR Arctic Viewer (2021) Marine geowissenschaftliche Daten—Projekt PANORAMA, https://arctic.bgr.de/mapapps4/resources/apps/arktis/index.html?lang=en (access date: 20.02.2024)

Blumenberg M, Weniger P, Kus J, Scheeder G, Piepjohn K, Zindler M, Reinhardt L (2018) Geochemistry of a middle Devonian cannel coal (Munindalen) in comparison with Carboniferous coals from Svalbard. Arktos 4(1):1–8. https://doi.org/10.1007/s41063-018-0038-y

Blumenberg et al. (2019) (Sub)-Bituminous coals from Svalbard and NE Greenland. Biomarkers hint at a closely related paleosetting during Paleogene, 29th annual meeting, Gothenburg, Sweden.

Blythe AE, Kleinspehn KL (1998) Tectonically versus climatically driven Cenozoic exhumation of the Eurasian plate margin, Svalbard: fission track analyses. Tectonics 17(4):621–639. https://doi.org/10.1029/98TC01890

Bordoloi M, Shukla VS, Nath SC, Sharma RP (1989) Naturally occurring cadinenes. Phytochemistry 28(8):2007–2037. https://doi.org/10.1016/S0031-9422(00)97915-9

Bourbonniere RA, Meyers PA (1996) Sedimentary geolipid records of historical changes in the watersheds and productivities of Lakes Ontario and Erie. Limnol Oceanogr 41(2):352–359. https://doi.org/10.4319/lo.1996.41.2.0352

Boyd A (1990) The thyra Ø flora: Toward an understanding of the climate and vegetation during the early tertiary in the high arctic. Rev Palaeobot Palynol 62(3–4):189–203. https://doi.org/10.1016/0034-6667(90)90089-2

Boyd A (1992) Musopsis n. gen.: A banana-like leaf genus from the early Tertiary of eastern North Greenland. Am J Bot. 79(12):1359–1367. https://doi.org/10.2307/2445134

Boyd A (2000) Paleogene paleoclimate of the North Atlantic Arctic as determined by vegetation. GFF 122(1):33. https://doi.org/10.1080/11035890001221033

Bruhn R, Steel R (2003) High-resolution sequence stratigraphy of a clastic foredeep succession (Paleocene, Spitsbergen): an example of peripheral-bulge-controlled depositional architecture. J Sediment Res 73(5):745–755. https://doi.org/10.1306/012303730745

Chaffee AL, Johns RB (1983) Polycyclic aromatic hydrocarbons in Australian coals. I. Angularly fused pentacyclic tri- and tetraaromatic components of Victorian brown coal. Geochim Cosmochim Acta 47(12):2141–2155. https://doi.org/10.1016/0016-7037(83)90039-X

Charles AJ, Condon DJ, Harding IC, Pälike H, Marshall JEA, Cui Y, Kump L, Croudace IW (2011) Constraints on the numerical age of the Paleocene-Eocene boundary. Geochem Geophys Geosyst. https://doi.org/10.1029/2010gc003426

Ćmiel SR, Fabiańska MJ (2004) Geochemical and petrographic properties of some Spitsbergen coals and dispersed organic matter. Int J Coal Geol 57(2):77–97. https://doi.org/10.1016/j.coal.2003.09.002

Dallmann WK (2015) Geoscience atlas of Svalbard. Rapportserie/Norsk Polarinstitutt, vol 148. Norsk Polarinstitutt, Tromsø

Denis EH, Toney JL, Tarozo R, Scott Anderson R, Roach LD, Huang Y (2012) Polycyclic aromatic hydrocarbons (PAHs) in lake sediments record historic fire events: validation using HPLC-fluorescence detection. Org Geochem 45:7–17. https://doi.org/10.1016/j.orggeochem.2012.01.005

Denis EH, Pedentchouk N, Schouten S, Pagani M, Freeman KH (2017) Fire and ecosystem change in the Arctic across the Paleocene-Eocene thermal maximum. Earth Planet Sci Lett 467:149–156. https://doi.org/10.1016/j.epsl.2017.03.021

Didyk BM, Simoneit BRT, Brassell SC, Eglinton G (1978) Organic geochemical indicators of palaeoenvironmental conditions of sedimentation. Nature 272(5650):216–222. https://doi.org/10.1038/272216a0

DIN 22020–3:1998–08, Rohstoffuntersuchungen im Steinkohlenbergbau_- Mikroskopische Untersuchungen an Steinkohle, Koks und Briketts_- Teil_3: Maceralanalysen an Körnerschliffen

DIN 22020–5:2005–02, Rohstoffuntersuchungen im Steinkohlenbergbau_- Mikroskopische Untersuchungen an Steinkohle, Koks und Briketts_- Teil_5: Reflexionsmessungen an Vitriniten

Dolezych M, Reinhardt L, Kus J, Annacker V (2019) Taxonomy of Cretaceous-Paleogene coniferous woods and their distribution in fossil Lagerstätten of the high latitudes. In: Piepjohn K, Strauss JV, Reinhardt L, Mc Clelland WC (eds) Circum-Arctic structural events: tectonic evolution of the Arctic margins and trans-arctic links with adjacent orogens. Geological Society of America, pp 9–44

Eglinton G, Murphy MTJ (eds) (1969) Organic geochemistry. Springer, Berlin, Heidelberg

Elling FJ, Spiegel C, Estrada S, Davis DW, Reinhardt L, Henjes-Kunst F, Allroggen N, Dohrmann R, Piepjohn K, Lisker F (2016) Origin of Bentonites and Detrital Zircons of the Paleocene Basilika Formation. Svalbard Front Earth Sci 4(73):1–23. https://doi.org/10.3389/feart.2016.00073

Ensminger A, Albrecht P, Ourisson G, Kimble BJ, Maxwell JR (1972) Homohopane in messel oil shale: first identification of a C31 pentacyclic triterpane in nature Bacterial origin of some triterpanes in ancient sediments. Tetrahedron Lett. 13(36):3861–3864. https://doi.org/10.1016/S0040-4039(01)94181-4

Espitalié J, Laporte JL, Madec M, Marquis F, Leplat P, Paulet J, Boutefeu A (1977) Méthode rapide de caractérisation des roches mètres, de leur potentiel pétrolier et de leur degré d'évolution. Rev Inst Fr Pét 32(1):23–42. https://doi.org/10.2516/ogst:1977002

Fabiańska MJ, Kurkiewicz S (2013) Biomarkers, aromatic hydrocarbons and polar compounds in the Neogene lignites and gangue sediments of the Konin and Turoszów Brown Coal Basins (Poland). Int J Coal Geol 107:24–44. https://doi.org/10.1016/j.coal.2012.11.008

Faleide JI, Vågnes E, Gudlaugsson ST (1993) Late Mesozoic-Cenozoic evolution of the south-western Barents Sea in a regional rift-shear tectonic setting. Mar Pet Geol 10(3):186–214. https://doi.org/10.1016/0264-8172(93)90104-Z

Fang R, Li M, Wang T-G, Zhang L, Shi S (2015) Identification and distribution of pyrene, methylpyrenes and their isomers in rock extracts and crude oils. Org Geochem 83–84:65–76. https://doi.org/10.1016/j.orggeochem.2015.03.003

Ficken K, Li B, Swain D, Eglinton G (2000) An n-alkane proxy for the sedimentary input of submerged/floating freshwater aquatic macrophytes. Org Geochem 31(7–8):745–749. https://doi.org/10.1016/S0146-6380(00)00081-4

Freeman KH, Pancost RD (2014) Biomarkers for terrestrial plants and climate. Treatise on geochemistry. Elsevier, New York, pp 395–416

Goossens H, de Leeuw JW, Schenck PA, Brassell SC (1984) Tocopherols as likely precursors of pristane in ancient sediments and crude oils. Nature 312(5993):440–442. https://doi.org/10.1038/312440a0

Gorbanenko O (2017) A dry polishing technique for the petrographic examination of mudrocks. Int J Coal Geol 180:122–126. https://doi.org/10.1016/j.coal.2017.03.013

Greenwood DR, Basinger JF, Smith RY (2010) How wet was the Arctic Eocene rain forest? Estimates of precipitation from Paleogene Arctic macrofloras. Geology 38(1):15–18. https://doi.org/10.1130/G30218.1

Haberer RM, Mangelsdorf K, Wilkes H, Horsfield B (2006) Occurrence and palaeoenvironmental significance of aromatic hydrocarbon biomarkers in Oligocene sediments from the Mallik 5L–38 Gas Hydrate Production Research Well (Canada). Org Geochem 37(5):519–538. https://doi.org/10.1016/j.orggeochem.2006.01.004

Håkansson E, Heinberg C, Stemmerik L (1991) Mesozoic and Cenozoic history of the Wandel Sea Basin area, North Greenland. In: Peel JS, Sønderholm M (eds) Sedimentary basins of North Greenland. Rapport Grønlands geologiske Undersøgelse. 160:153–164. https://doi.org/10.34194/bullggu.v160.6716

Huang W-Y, Meinschein WG (1979) Sterols as ecological indicators. Geochim Cosmochim Acta 43(5):739–745. https://doi.org/10.1016/0016-7037(79)90257-6

ICCP (1998) The new vitrinite classification (ICCP System 1994). Fuel 77(5):349–358. https://doi.org/10.1016/S0016-2361(98)80024-0

ICCP (2001) The new inertinite classification (ICCP System 1994). Fuel 80(4):459–471. https://doi.org/10.1016/S0016-2361(00)00102-2

ISO 7404–2 (2009) Methods for the petrographic analysis of coals—part 2: methods of preparing coal samples. International Organization for Standardization, Geneva, Switzerland. pp 12. https://www.iso.org/standard/42798.html

ISO 7404–3 (2009) Methods for the petrographic analysis of bituminous coal and anthracite—part 3: Method of determining maceral group composition, first ed. International Organization for Standardization, Geneva, Switzerland. pp 7. https://www.iso.org/standard/42831.html

ISO 7404–5 (2009) Methods for the petrographic analysis of coals—part 5: method of determining microscopically the reflectance of vitrinite, third ed. International Organization for Standardization, Geneva, Switzerland. pp 14. https://www.iso.org/standard/42832.html

Izart A, Suarez-Ruiz I, Bailey J (2015) Paleoclimate reconstruction from petrography and biomarker geochemistry from Permian humic coals in Sydney Coal Basin (Australia). Int J Coal Geol 138:145–157. https://doi.org/10.1016/j.coal.2014.12.009

Jochmann MM, Augland LE, Lenz O, Bieg G, Haugen T, Grundvåg SA, Jelby ME, Midtkandal I, Dolezych M, Hjálmarsdóttir HR (2020) Sylfjellet: a new outcrop of the Paleogene Van Mijenfjorden Group in Svalbard. Arktos 6(1–3):17–38. https://doi.org/10.1007/s41063-019-00072-w

Jones MT, Eliassen GT, Shephard GE, Svensen HH, Jochmann M, Friis B, Augland LE, Jerram DA, Planke S (2016) Provenance of bentonite layers in the Palaeocene strata of the Central Basin, Svalbard: implications for magmatism and rifting events around the onset of the North Atlantic Igneous Province. J Volcanol Geoth Res 327:571–584. https://doi.org/10.1016/j.jvolgeores.2016.09.014

Jones MT, Augland LE, Shephard GE, Burgess SD, Eliassen GT, Jochmann MM, Friis B, Jerram DA, Planke S, Svensen HH (2017) Constraining shifts in North Atlantic plate motions during the Palaeocene by U-Pb dating of Svalbard tephra layers. Sci Rep 7(1):6822. https://doi.org/10.1038/s41598-017-06170-7

Kalaitzidis S, Bouzinos A, Christanis K (2000) The lignite-forming palaeoenvironment before and after the volcanic tephra deposition in the Ptolemais basin, Hellas. Mineral Wealth 115:29–42

Killops S, Killops V (2004) Introduction to organic geochemistry, 2nd edn. Blackwell Publishing Ltd, Malden

Konrad W, Roth-Nebelsick A, Traiser C (2023) High productivity at high latitudes. Photosynthesis and leaf ecophysiology in Arctic

forests of the eocene. Paleoceanogr Paleoclimatol. https://doi.org/10.1029/2023PA004685
Kus J, Dolezych M, Schneider W, Hofmann T, Rajczi V (2020) Coal petrological and xylotomical characterization of Miocene lignites and in-situ fossil tree stumps and trunks from Lusatia region, Germany: Palaeoenvironment and taphonomy assessment. Int J Coal Geol 217:103283. https://doi.org/10.1016/j.coal.2019.103283
Lafargue E, Marquis F, Pillot D (1998) Rock-eval 6 applications in hydrocarbon exploration, production, and soil contamination studies. Rev Inst Fr Pét 53(4):421–437. https://doi.org/10.2516/ogst:1998036
Lawver LA, Müller RD, Srivastava SP, Roest W (1990) The opening of the Arctic Ocean. In: Bleil U, Thiede J (eds) Geological history of the polar oceans: Arctic versus Antarctic. Springer, Netherlands, Dordrecht, pp 29–62
Li M, Wang T, Zhong N, Zhang W, Sadik A, Li H (2013) Ternary diagram of fluorenes, dibenzothiophenes and dibenzofurans: indicating depositional environment of crude oil source rocks. Energy Explor Exploit 31(4):569–588. https://doi.org/10.1260/0144-5987.31.4.569
Logan GA, Smiley CJ, Eglinton G (1995) Preservation of fossil leaf waxes in association with their source tissues, Clarkia, northern Idaho, USA. Geochim Cosmochim Acta 59(4):751–763. https://doi.org/10.1016/0016-7037(94)00362-P
Lyck JM, Stemmerik L (2000) Palynology and depositional history of the Paleocene. Thyra Ø Formation, Wandel Sea Basin, eastern North Greenland. Bull Geol Surv Greenland 187:21–49. https://doi.org/10.34194/ggub.v187.5193
Manum SB, Throndsen T (1986) Age of tertiary formations on Spitsbergen. Polar Res 4(2):103–131. https://doi.org/10.3402/polar.v4i2.6927
Marshall C (2013) Palaeogeographic development and economic potential of the coal-bearing palaeocene Todalen Member, Spitsbergen. Dissertation, University of Nottingham.
Marshall C, Large DJ, Meredith W, Snape CE, Uguna C, Spiro BF, Orheim A, Jochmann M, Mokogwu I, Wang Y, Friis B (2015a) Geochemistry and petrology of Palaeocene coals from Spitsbergen—part 1: oil potential and depositional environment. Int J Coal Geol 143:22–33. https://doi.org/10.1016/j.coal.2015.03.006
Marshall C, Uguna J, Large DJ, Meredith W, Jochmann M, Friis B, Vane C, Spiro BF, Snape CE, Orheim A (2015b) Geochemistry and petrology of palaeocene coals from Spitzbergen—part 2: maturity variations and implications for local and regional burial models. Int J Coal Geol 143:1–10. https://doi.org/10.1016/j.coal.2015.03.013
Marynowski L, Simoneit BRT (2009) Widespread upper triassic to lower Jurassic wildfire records from poland: evidence from charcoal and pyrolytic polycyclic aromatic hydrocarbons. Palaios 24(12):785–798. https://doi.org/10.2110/palo.2009.p09-044r
Marynowski L, Czechowski F, Simoneit BR (2001) Phenylnaphthalenes and polyphenyls in Palaeozoic source rocks of the Holy Cross Mountains. Poland Org Geochem 32(1):69–85. https://doi.org/10.1016/S0146-6380(00)00150-9
Marynowski L, Smolarek J, Hautevelle Y (2015) Perylene degradation during gradual onset of organic matter maturation. Int J Coal Geol 139:17–25. https://doi.org/10.1016/j.coal.2014.04.013
Marzi R, Torkelson BE, Olson RK (1993) A revised carbon preference index. Org Geochem 20(8):1303–1306. https://doi.org/10.1016/0146-6380(93)90016-5
Meyer W, Seiler T-B, Christ A, Redelstein R, Püttmann W, Hollert H, Achten C (2014) Mutagenicity, dioxin-like activity and bioaccumulation of alkylated picene and chrysene derivatives in a German lignite. Sci Total Environ 497–498:634–641. https://doi.org/10.1016/j.scitotenv.2014.07.103
Myhre AM, Eldholm O (1988) The western Svalbard margin (74°–80°N). Mar Pet Geol 5(2):134–156. https://doi.org/10.1016/0264-8172(88)90019-0
NOAA (2019) NOAA esri ArcGi; https://gis.ngdc.noaa.gov/arcgis/rest/services/DEM_mosaics/DEM_global_mosaic/ImageServer. Accessed Sep 2019
Noble RA, Alexander R, Kagi RI, Knox J (1985) Tetracyclic diterpenoid hydrocarbons in some Australian coals, sediments and crude oils. Geochim Cosmochim Acta 49(10):2141–2147. https://doi.org/10.1016/0016-7037(85)90072-9
Noble RA, Alexander R, Kagi RI, Nox JK (1986) Identification of some diterpenoid hydrocarbons in petroleum. Org Geochem 10(4–6):825–829. https://doi.org/10.1016/S0146-6380(86)80019-5
Nott CJ, Xie S, Avsejs LA, Maddy D, Chambers FM, Evershed RP (2000) n-Alkane distributions in ombrotrophic mires as indicators of vegetation change related to climatic variation. Org Geochem 31(2–3):231–235. https://doi.org/10.1016/S0146-6380(99)00153-9
ODSN (2022) ODSN Plate Tectonic Reconstruction Service; https://www.odsn.de/odsn/services/paleomap/paleomap.html. Accessed 30 Mar 2022
O'Keefe JMK, Bechtel A, Christianis K, Dai S, DiMichele WA, Eble CF, Esterle JS, Mastalerz M, Raymond AL, Valentim BV, Wagner NJ, Ward CR, Hower JC (2013) On the fundamental difference between coal rank and coal type. Int J Coal Geol 118:58–87. https://doi.org/10.1016/j.coal.2013.08.007
Orheim A, Bieg G, Brekke T, Horseide V, Stenvold J (2007) Petrography and geochemical affinities of Spitsbergen Paleocene coals. Norway Int J Coal Geol 70(1–3):116–136. https://doi.org/10.1016/j.coal.2006.04.008
Otto A, Simoneit BR (2001) Chemosystematics and diagenesis of terpenoids in fossil conifer species and sediment from the Eocene Zeitz formation, Saxony. Germany Geochim Cosmochim Acta 65(20):3505–3527. https://doi.org/10.1016/S0016-7037(01)00693-7
Otto A, Wilde V (2001) Sesqui-, di-, and triterpenoids as chemosystematic markers in extant conifers—A review. Bot Rev 67(2):141–238. https://doi.org/10.1007/bf02858076
Otto A, Simoneit BR, Rember WC (2005) Conifer and angiosperm biomarkers in clay sediments and fossil plants from the Miocene Clarkia Formation, Idaho, USA. Org Geochem 36(6):907–922. https://doi.org/10.1016/j.orggeochem.2004.12.004
Otto A, Gondokusumo R, Simpson MJ (2006) Characterization and quantification of biomarkers from biomass burning at a recent wildfire site in Northern Alberta. Canada Appl Geochem 21(1):166–183. https://doi.org/10.1016/j.apgeochem.2005.09.007
Ourisson G, Albrecht P, Rohmer M (1979) The Hopanoids: palaeochemistry and biochemistry of a group of natural products. Pure Appl Chem 51(4):709–729. https://doi.org/10.1351/pac197951040709
Ourisson G, Albrecht P, Rohmer M (1984) The microbial origin of fossil fuels. Sci Amer 251(2):44–51. https://doi.org/10.1038/scientificamerican0884-44
Paech H-J, Estrada S (2019) Coal rank data and tectonic structure of Mesozoic and Paleogene sediments in North Greenland. In: Piepjohn K, Strauss JV, Reinhardt L, McClelland WC (eds) Circum-Arctic Structural Events: Tectonic Evolution of the Arctic Margins and Trans-Arctic Links with Adjacent Orogens. Geological Society of America, pp 189–211
Parkes RJ, Taylor J (1983) The relationship between fatty acid distributions and bacterial respiratory types in contemporary marine sediments. Estuar Coast Shelf Sci 16(2):173–189. https://doi.org/10.1016/0272-7714(83)90139-7

Peters KE (1986) Guidelines for evaluating petroleum source rock using programmed pyrolysis. AAPG Bull. https://doi.org/10.1306/94885688-1704-11D7-8645000102C1865D

Peters KE, Walters CC, Moldowan JM (2005) The Biomarkers Guide. Biomarkers and isotopes in the environment and human history, vol. 2, 2. ed., reprinted with corrections, digitally printed version 2005. Peters KE, Walters CC, Moldowan JM (eds) The biomarker guide 2. Cambridge Univ. Press, Cambridge, UK [u.a.]

Piasecki S, Nøhr-Hansen H, Dalhoff F (2018) Revised stratigraphy of Kap Rigsdagen beds, Wandel Sea Basin, North Greenland. Newsl Stratigr 51(4):411–425. https://doi.org/10.1127/nos/2018/0444

Philp RP (1985) Fossil fuel biomarkers. Elsevier Science Pub. Co. Inc, New York

Pickel W, Kus J, Flores D, Kalaitzidis S, Christanis K, Cardott BJ, Misz-Kennan M, Rodrigues S, Hentschel A, Hamor-Vido M, Crosdale P, Wagner N (2017) Classification of liptinite—ICCP System 1994. Int J Coal Geol 169:40–61. https://doi.org/10.1016/j.coal.2016.11.004

Piepjohn K, von Gosen W, Tessensohn F (2016) The Eurekan deformation in the Arctic: an outline. JGS 173(6):1007–1024. https://doi.org/10.1144/jgs2016-081

Poinar G, Archibald B, Brown A (1999) New amber deposit provides evidence of Early Paleogene extinctions, paleoclimates, and past distributions. Can Entomologist 131(2):171–177. https://doi.org/10.4039/Ent131171-2

Radke M, Welte DH, Willsch H (1986) Maturity parameters based on aromatic hydrocarbons: influence of the organic matter type. Org Geochem 10(1–3):51–63. https://doi.org/10.1016/0146-6380(86)90008-2

Rowland SJ, Alexander R, Kagi RI (1984) Analysis of trimethylnaphthalenes in petroleum by capillary gas chromatography. J Chromatogr A 294:407–412. https://doi.org/10.1016/S0021-9673(01)96153-9

Ruddiman WF (2014) Earth's climate. Past and future, 3rd edn. W. H. Freeman and Company, New York

Scalan E, Smith J (1970) An improved measure of the odd-even predominance in the normal alkanes of sediment extracts and petroleum. Geochim Cosmochim Acta 34(5):611–620. https://doi.org/10.1016/0016-7037(70)90019-0

Schlanser KM, Diefendorf AF, West CK, Greenwood DR, Basinger JF, Meyer HW, Lowe AJ, Naake HH (2020) Conifers are a major source of sedimentary leaf wax n-alkanes when dominant in the landscape: case studies from the Paleogene. Org Geochem 147:1–17. https://doi.org/10.1016/j.orggeochem.2020.104069

Schweitzer H-J (1980) Environment and climate in the early tertiary of Spitsbergen. Palaeogeogr Palaeoclimatol Palaeoecol 30:297–311. https://doi.org/10.1016/0031-0182(80)90062-0

Seifert WK, Michael Moldowan J (1978) Applications of steranes, terpanes and monoaromatics to the maturation, migration and source of crude oils. Geochim Cosmochim Acta 42(1):77–95. https://doi.org/10.1016/0016-7037(78)90219-3

Simoneit BR (1977) Diterpenoid compounds and other lipids in deep-sea sediments and their geochemical significance. Geochim Cosmochim Acta 41(4):463–476. https://doi.org/10.1016/0016-7037(77)90285-X

Simoneit BR, Grimalt JO, Wang TG, Cox RE, Hatcher PG, Nissenbaum A (1986) Cyclic terpenoids of contemporary resinous plant detritus and of fossil woods, ambers and coals. Org Geochem 10(4–6):877–889. https://doi.org/10.1016/S0146-6380(86)80025-0

Simoneit BR, Mazurek MA (1982) Organic matter of the troposphere—II. Natural background of biogenic lipid matter in aerosols over the rural western united states. Atmos Environ. 16(9):2139–2159. https://doi.org/10.1016/0004-6981(82)90284-0

Sluijs A, Schouten S, Pagani M, Woltering M, Brinkhuis H, Sinninghe Damsté JS, Dickens GR, Huber M, Reichart G-J, Stein R, Matthiessen J, Lourens LJ, Pedentchouk N, Backman J, Moran K (2006) Subtropical Arctic Ocean temperatures during the Palaeocene/Eocene thermal maximum. Nature 441(7093):610–613. https://doi.org/10.1038/nature04668

Stemmerik L, Dalhoff F, Larsen BD, Lyck J, Mathiesen A, Nilsson I (1998) Wandel Sea Basin, eastern North Greenland. Geol Greenl Surv Bull 180:55–62. https://doi.org/10.34194/ggub.v180.5086

Stout SA (1992) Aliphatic and aromatic triterpenoid hydrocarbons in a Tertiary angiospermous lignite. Org Geochem 18(1):51–66. https://doi.org/10.1016/0146-6380(92)90143-L

Strachan MG, Alexander R, Kagi RI (1988) Trimethylnaphthalenes in crude oils and sediments: effects of source and maturity. Geochim Cosmochim Acta 52(5):1255–1264. https://doi.org/10.1016/0016-7037(88)90279-7

Taylor GH, Teichmüller M, Davis A, Diessel CFK, Littke R, Robert P (1998) Organic Petrology. A New Handbook incorporating some revised parts of Stach's Textbook of Coal Petrology. Berlin, Stuttgart: Gebrüder Borntraeger. https://doi.org/10.1017/S0016756899463320

Tessensohn F, Piepjohn K (2000) Eocene compressive deformation in Arctic Canada, North Greenland and Svalbard and its plate tectonic causes. Polarforschung 68(68):121–124

ten Haven HL, de Leeuw JW, Rullkötter J, Damsté JSS (1987) Restricted utility of the pristane/phytane ratio as a palaeoenvironmental indicator. Nature 330(6149):641–643. https://doi.org/10.1038/330641a0

Thiäner JB, Nett L, Zhou S, Preibisch Y, Hollert H, Achten C (2019) Identification of 7–9 ring polycyclic aromatic hydrocarbons in coals and petrol coke using High performance liquid chromatography—diode array detection coupled to atmospheric pressure laser ionization—mass spectrometry (HPLC-DAD-APLI-MS). Environ Pollut 252(Pt A):723–732. https://doi.org/10.1016/j.envpol.2019.05.109

Tissot BP, Welte DH (1984) Petroleum Formation and Occurrence, 2nd edn. Springer-Verlag, Berlin

van Aarssen BG, Alexander R, Kagi RI (2000) Higher plant biomarkers reflect palaeovegetation changes during Jurassic times. Geochim Cosmochim Acta. 64(8):1417–1424. https://doi.org/10.1016/S0016-7037(99)00432-9

van Krevelen DW (1993) Coal. Typology, physics, chemistry, constitution, 3rd edn. Elsevier, Amsterdam

Volkman JK (2005) Sterols and other triterpenoids: source specificity and evolution of biosynthetic pathways. Org Geochem 36(2):139–159. https://doi.org/10.1016/j.orggeochem.2004.06.013

Wakeham SG, Canuel EA (2016) Biogenic polycyclic aromatic hydrocarbons in sediments of the San Joaquin River in California (USA), and current paradigms on their formation. Environ Sci Pollut Res 23(11):10426–10442. https://doi.org/10.1007/s11356-015-5402-x

Weijers JW, Schouten S, Sluijs A, Brinkhuis H, Sinninghe Damsté JS (2007) Warm arctic continents during the Palaeocene-Eocene thermal maximum. Earth Planet Sci Lett 261(1–2):230–238. https://doi.org/10.1016/j.epsl.2007.06.033

West CK, Greenwood DR, Basinger JF (2015) Was the Arctic Eocene 'rainforest' monsoonal? Estimates of seasonal precipitation from early Eocene megafloras from Ellesmere Island, Nunavut. Earth Planet Sci Lett 427:18–30. https://doi.org/10.1016/j.epsl.2015.06.036

Widodo S, Bechtel A, Anggayana K, Püttmann W (2009) Reconstruction of floral changes during deposition of the Miocene Embalut coal from Kutai Basin, Mahakam Delta, East Kalimantan, Indonesia by use of aromatic hydrocarbon composition and stable carbon isotope ratios of organic matter. Org Geochem 40(2):206–218. https://doi.org/10.1016/j.orggeochem.2008.10.008